2017

Vitamin D3 and Suppressor of Cytokine Signaling Proteins Reduces Pro-Inflammatory Cytokines in an Alzheimer's Disease Like-Model Consisting of Microglial and Neuronal Co-Cultures

Alexander Evdokiou
Wright State University

Vitamin D3 and Suppressor of Cytokine Signaling Proteins Reduces Pro-Inflammatory Cytokines in an Alzheimer's Disease Like-Model Consisting of Microglial and Neuronal Co-Cultures

A thesis submitted in partial fulfillment

of the requirement for the degree of

Master of Science.

By

Alexander Evdokiou

B.S., University of Cincinnati, 2015

2017

Wright State University

Wright State University

Graduate School

July 19,2017

I HEREBY RECOMMEND THAT THE THESIS PREPARED UNDER MY SUPERVISION BY ALEXANDER EVDOKIOU ENTITILED Vitamin D3 and Suppressor of Cytokine Signaling Proteins Reduces Pro-Inflammatory Cytokines in an Alzheimer's Disease Like-Model Consisting of Microglial and Neuronal Co-Cultures BE ACCEPTED IN PARTIAL FULFILLMENT OF THE REQUIREMENTS FOR THE DEGREEE OF Master of Science.

Committee on Final Examination

Nancy J. Bigley Ph.D.
Thesis Director

Nancy J. Bigley, Ph.D.
Professor of Neuroscience, Cell Biology, and Physiology

Barbara E. Hull, Ph.D.
Director of Microbiology and Immunology Program, College of Science and Mathematics

Barbara E. Hull, Ph.D.
Professor of Biological Sciences

Shulin Ju, Ph.D.
Assistant Professor of Biological Sciences

Robert E.W. Fyffe, Ph.D.
Vice President for Research and Dean of the Graduate School

ABSTRACT

Evdokiou, Alexander. M.S. Department of Microbiology and Immunology, Wright State University, 2017. Vitamin D3 and Suppressor of Cytokine Signaling Proteins Reduces Pro-Inflammatory Cytokines in an Alzheimer's Disease Like-Model Consisting of Microglial and Neuronal Co-Cultures.

This study examined the inflammatory effects of amyloid-β (Aβ42) in a microglial-neuronal co-culture system and determined whether 1α, 25-dihydroxyvitamin D3 (1,25-(OH)2D3) along with suppressor of cytokine signaling (SOCS)1 and SOCS 3 mimetics would attenuate the inflammatory response to Aβ42. This culture system, when seeded with Aβ42, serves as an *in vitro* model for Alzheimer's disease (AD). In a neuronal-microglia co-culture, Aβ42 stimulated microglia to secrete TNF-α, but with the addition of 1,25-(OH)2D3, TNF-α levels dropped by nearly eight-fold and to near zero values in the presence of both 1,25-(OH)2D3 and SOCS1 and SOCS 3 mimetics. The reduction of the inflammatory cytokine TNF-α by both 1,25-(OH)2D3 and SOCS mimetics, suggests that these molecules may be an effective means of treating AD related inflammation, and that 1,25-(OH)2D3 along with SOCS proteins mimetics should be considered for early onset AD.

Table of Contents

List of Figures

List of Tables

List of Abbreviations

1,25-(OH)2D3= 1 α,25-dihydroxyvitaminD3

Aβ42= Amyloid-β

AD= Alzheimer's Disease

ApoE= Apolipoprotein E

APP= Amyloid Precursor Protein

BACE1= Beta-secretase 1

BBB= Blood Brain Barrier

DMEM= Dulbecco's Modified Eagle Medium

FBS= Fetal Bovine Serum

IFN-γ= Interferon gamma

IL-10= Interluekin-10

JAK= Janus Kinase

LPS= Lipopolysaccharide (*Escherichia coli)*

N2A= Neruo-2A neurons

RXR= Retinoid X Receptor

SIM= Spontaneously immortalized Microglia

SOCS= Suppressor of Cytokine Signaling

STAT= Signal Transducers and Activators of Transcription

TLR= Toll Like Receptor

TNF-α= Tumor Necrosis Factor-α

VD3= Vitamin D3

VDR= Vitamin D Receptor

VDRE= Vitamin D Response Element

Acknowledgment

I would like to express my sincerest gratitude to Dr. Nancy Bigley for all her time and support. I came to Dr. Bigley with a new idea for a thesis project, and she graciously allowed me to pursue my interests. All my work would not be possible without her guidance. I would like to thank Dr. Barbara Hull for always letting me come to her office to ask questions or for guidance during my experiments. Dr. Hull's courses were some of my favorites, where I learned a great deal about what it meant to do research. I would also like to thank Dr. Shulin Ju for sitting on this committee and for his insights into neurodegenerative disorders. With his knowledge, my thesis has become a more well-rounded product. Thank you as well to my friends in the Bigley lab, who made getting my degree incredibly fun. Lastly, thank you to Rebecca and to my family who I have leaned on heavily over the past two years.

Introduction

Alzheimer's Disease (AD) is a neurodegenerative disorder that affects nearly 5 million people in the United States (Hebert et al., 2013). The total number of Americans with AD is predicted to reach approximately 14 million people by the year 2050 (Hebert et al., 2013). One singular cause for the disease is not known; however, amyloid-β (Aβ) has been found to play a large role in the pathology of AD (O'Brien et al., 2011). Aβ42 is involved in synaptic plasticity and neuronal health, but changes in the expression of Aβ42 result in a disease state (Puzzo et al., 2008). As concentrations of Aβ42 rise to nanomolar or micromolar levels, aggregates of Aβ42 form in the brain (Combs et al., 2001; Cardenas-Aguayo et al., 2014). The mechanism by which these plaques arise is unknown, but their effect is such that neurons become starved, proper signaling is diminished, and the cells eventually die. These plaques of Aβ42 cause an immune response, with the main effector cell being microglia. Microglia are the resident macrophage of the central nervous system (CNS). In a non-inflamed CNS, microglia are kept in circulation, where they maintain a fairly even ratio of M1 to M2 microglia. Microglia interact directly with extracellular aggregated Aβ42, through toll like receptor (TLR) 4 (Joshi et al., 2014), which activates a pro-inflammatory response and the release of cytokines such as TNF-α from microglia (Combs et al., 2001). Therefore, in AD, an overproduction of Aβ42 results in the production of pro-inflammatory cytokines and inflammation in the brains of AD patients.

AD is a progressive neurological disorder, that worsens severely with age. An early, preventative measure to counter the neuroinflammation in AD could help to reduce symptoms from becoming worse. A candidate for this preventative measure is Vitamin D3 (VD3), which has many anti-inflammatory properties. The active form of VD3, 1α, 25-dihydroxyvitamin D3 (1,25-(OH)2D3), is the most effective anti-inflammatory form of VD3. Previous studies have shown that, following activation of the inflammatory response, 1,25-(OH)2D3 was able to shift microglial activation away from M1 towards the anti-inflammatory M2 (Boontanrart et al., 2016). In doing so, the presence of pro-inflammatory cytokines decreases, while the concentration of anti-inflammatory cytokines increases (Boontanrart et al., 2016). 1,25-(OH)2D3 inhibits the inflammatory response by preventing NF-κB signaling. NF-κB is a complex of proteins, that has been shown to act as a strong inducer of the inflammatory response (Tak and Firestein, 2001; Yoshimura et al., 2007; Lawrence, 2009). The entire complex acts as a transcription factor to upregulate transcription of M1 cytokines and to initiate the inflammatory response. 1,25-(OH)2D3 can directly bind to this complex to prevent the translocation of NF-κB into the nucleus. Along with 1,25-(OH)2D3, SOCS1 can also directly bind to NF-κB to prevent translocation of the complex to the nucleus. SOCS3 prevents the complex of TRAF-6 and TAK1 from activating the NF-κB complex (Yoshimura et al., 2007). In this study, 1,25-(OH)2D3 and SOCS mimetics successfully reduced Aβ42 induced TNF-α secretion ($p<0.05$). In concert, 1,25-(OH)2D3 and SOCS mimetics reduced Aβ42 induced TNF-α secretion to near zero values ($p<0.05$). With supplements found readily over the counter, VD3 could serve as an excellent means to slow early inflammation in an early onset AD brain.

Literature Review

This review is focused on describing the possible underlying mechanisms of amyloid-β (Aβ42)-related inflammation. These mechanisms include Aβ42 aggregation, amyloid precursor protein splicing, miRNA-dependent gene expression of the amyloid precursor protein and β-secretase, transport, and clearance of Aβ42, and mutations within apolipoprotein E. Also included are the innate functions of microglia, suppresser of cytokine signaling, and vitamin D and how they have been studied in inflammation.

The synthesis of Aβ42 is crucial to understanding AD pathology. Aβ42 arises from secretase activity on its precursor, the amyloid precursor protein (APP) (Chow et al., 2010; O'Brien et al., 2011). Aβ42 is released from the APP and, in AD, this activity is increased. An increase in the concentration of Aβ42 results in plaque formation, called aggregates (Maezawa et al., 2010). These aggregates of Aβ42 are a strong inducer of the inflammatory response (Sengupta et al., 2016). The resident phagocytic cell of the CNS, microglia, are unable to process the plaques and, in response, they secrete pro-inflammatory cytokines. Over the years of AD progression, this inflammation continually increases (Martorana et al., 2012). Questions remain over how Aβ42 would cause AD. The most supported theory is the amyloid cascade theory which states that Aβ42 aggregation does not directly cause AD but does begin a cascade of inflammation and misfolded proteins that may lead to AD (Karran et al., 2011). At the heart of this theory is the inflammatory response to aggregated Aβ42. This review will describe two

means of controlling this inflammation: suppressor of cytokine signaling (SOCS) proteins and Vitamin D3 (VD3). SOCS proteins function to inhibit cytokine signaling and have been shown to reduce pro-inflammatory cytokines. The active metabolite of VD3, 1,25-(OH)2D3, has been shown to possess potent anti-inflammatory properties (Boontanrart et al., 2016). With the ability to cross the blood brain barrier (BBB), 1,25-(OH)2D3 is a candidate for reducing neuro-inflammation in AD. This review will cover how Aβ42 plays a large role in AD, and how these negative effects of Aβ42 may be controlled using SOCS proteins and VD3.

The Amyloid Precursor Protein (APP)

The APP is a single-pass transmembrane protein with extracellular domains (O'Brien et al., 2011). Within the full length of the APP is Aβ42, which must first be spliced by several enzymes to be released. Once the APP reaches the cell surface, it can then be spliced by several secretases. However, only a single pathway leads to the creation of Aβ. Full length APP is initially cleaved by α-secretase or β-secretase, although α-secretase activity does not result in Aβ production. If the APP is cleaved by β-secretase (BACE1, an aspartyl protease (Pearson et al.,2006)), the splice site for γ-secretase is made available, which results in the release of three proteins: soluble APP beta (sAPPβ), the amyloid precursor protein intracellular domain (AICD), and Aβ (Zhang et al., 2011). sAPPβ functions as a death receptor ligand, mediates axon shortening, and neuronal cell death (Mills and Reiner, 1999). The AICD remains within the cell, and can impair mitochondrial functions. The oxidative stress that results from dysregulated mitochondrial function, has been shown to increase oxidative stress and inflammation (Ward, 2010). This oxidative stress increases the inflammation seen in AD and disease

progression. Therefore, a potential cause of Aβ42-related AD is alternative splicing of the APP. In mice, knockout of the APP gene has been shown to result in deformities, decreased brain size, decreased ratio of surface area to volume of brains, and underdeveloped brains were common phenotypes (Ring et al., 2007). Clearly, the presence of the APP is necessary for normal development, so downstream proteins or enzymes must be targeted as potential treatments for inappropriate alternative splicing of the APP.

The expression of the APP and its post-transcriptional modifications are two other avenues of research for AD treatment. Researchers have shown that downregulation of miRNA-124 expression was more commonly found in AD patients (Smith et al., 2011). This group showed that miR-124 normally functions to bind the transcripts for the APP, thereby controlling the expression of Aβ42 (Smith et al., 2011). Without mi-124, APP is more highly expressed, and, following secretase activity, Aβ42 concentrations are increased. miRNAs also play a role in controlling the expression of BACE1. If miR-29a/b1 is present, BACE1 expression is decreased because this miRNA specifically binds the transcripts responsible for BACE1 (Hebert et al., 2008). In the same study, miR-29a/b1 levels were also found to be decreased in AD patients (Hebert et al., 2008). In another study, AD transgenic mice with reduced BACE1 expression showed increased learning and memory, both of which diminish in AD, suggesting that BACE1 plays a large role in the progression of worsening symptoms in AD. (Kimura et al., 2010). To substantiate this claim, Coulson et al. (2010) studied the post-mortem brains of AD patients to determine the mRNA levels of BACE1. This group found that brains of AD patients contained increased levels of BACE1 mRNA. Furthermore, in a transgenic

mouse model of AD with a single BACE1 allele knocked out, (Kimura et al., 2010), levels of both Aβ40 and Aβ42 were significantly reduced and plaque formation was decreased. The decrease in Aβ suggests that an inhibitor for BACE1 may be a potential therapeutic target for AD.

Amyloid-β (Aβ42)

Aβ42 has been implicated in the pathogenesis of AD since its isolation from AD patient brains by Genner and Wong (1984). Since then, a large effort has been made to understand Aβ42 and how the presence of Aβ42 plaques leads to AD. For many years, researchers puzzled over the fact that the presence of plaques did not always correlate with increased patient dementia (Murphy et al., 2011). Now, it is understood that both the concentration of Aβ42 and its solubility plays a large role in AD progression. Aβ42 exists in two major isoforms, Aβ40 and Aβ42 (Tapiola et al., 2009; Bibl et al., 2012). The ratio of Aβ42: Aβ40 is currently being used as an AD-biomarker, with a high ratio correlating to a higher likelihood of developing AD (Bibl et al., 2012). In a healthy brain, the relative ratio of Aβ42: Aβ40 is approximately 1:10 (Deane et al., 2009). However, in AD neurons, this ratio rises because of the sequestering of Aβ42 by plaque formation (Hansson et al., 2007; Deane et al., 2009). These plaques are insoluble aggregates and are attractants for microglia. Unable to destroy the aggregates, microglia release chemoattractants and cytokines that result in edema and prolonged inflammation in the CNS. As the number of plaques increase, so does the inflammation (Martorana et al., 2012). This may explain the progressive nature of AD. Chronic inflammation can lead to heart failure, arthritis, and many other issues. Therefore, AD should be treated as an

inflammatory disease and requires attention in controlling the inflammatory response (Hong et al., 2016; Heneka et al., 2015).

Microglia are critical in the development of AD. Understanding their interaction with Aβ42 will aid in determining effective means of treating AD. Microglia interact with Aβ42 through toll-like receptor (TLR)-4 (Lehnardt et al., 2002; Walter et al., 2007), and through MAPK signaling cascades to increase transcription of M1 cytokines such as TNF-α (Heneka et al., 2012). Extracellular TNF-α secreted from microglia triggers further inflammation and edema in the brain. However, only insoluble aggregates of Aβ42 cause this reaction. Aβ42 is required for proper synaptic plasticity and neuronal health (Plant et al., 2003). Plant et al. (2003) determined that secretase inhibitors or anti-Aβ42 antibodies significantly increased rat neuronal death. Astrocytes and other cell types remained viable in the presence of both secretase inhibitors and antibody, suggesting that the effects of Aβ42 are neuron-specific. Cells treated with secretase inhibitors could be rescued by the addition of Aβ42, where significant increase in viability was detected (Plant et al., 2003). This work shows that, while Aβ42 is clearly implicated in AD, removal of Aβ42 is not a therapeutic target for treating patients with AD.

If Aβ42 is crucial to neuronal health, but aggregates of Aβ42 cause severe inflammation, then it is thought that changes in transport and clearance of Aβ42 are crucial to AD development. Mutations in transport proteins such as apolipoprotein E (ApoE) could serve as a strong biomarker for AD. ApoE is a transport molecule that is responsible for the clearance of Aβ42 into the blood stream for degradation and removal (Deane et al., 2009). Mutations in this transport protein have recently been considered a

top candidate for the increase in Aβ42 concentrations in AD (Morris et al., 2010). Using CSF from patients with a mutated ApoE2 allele, it was found that these patients had higher CSF concentrations of Aβ42 (Morris et al., 2010). The concentration of AB42 in CSF was higher with increasing age as well. Not only do older individuals suffer from more chronic inflammation, but this inflammation would be coupled with an increase in Aβ42 concentrations within brain tissue, and increasing the probability of aggregation formation. Morris et al. (2010) state that only Aβ42 pathology is related to mutations in ApoE and it has been previously shown that Aβ42 does not directly cause the disease state seen in AD. The amyloid cascade theory is currently the most supported model for predicting the mechanism by which Aβ42 could result in AD (Karren et al., 2011; McGeer et al., 2013).

The Amyloid Cascade Theory

As more Aβ42 is generated, aggregation formation, inflammation and stress cause changes within the cell. As Aβ42 concentrations reach nanomolar or micromolar concentrations, monomers tend to form large aggregate pools. The "Amyloid Cascade Theory" states that Aβ42 alone is not what causes AD, but rather begins a detrimental cascade of improper protein folding that leads to the onset of AD (Karran et al., 2011). In the beginning, most likely due to genetic mutations, extracellular levels of Aβ42 levels start to rise. Friedrich et al. (2009) studied how Aβ42 aggregation may begin. Their study showed that initially, Aβ42 is phagocytosed and housed in vesicles. Within vesicles, Aβ42 monomers form structured oligomers, putting stress of the vesicle walls. Eventually, the rigid structure of Aβ42 oligomers causes vesicles to rupture, releasing Aβ42 oligomers into the cytosol of the cell. In this *in vitro* model, extensive cell death

was reported following this release of Aβ42 oligomers. Following cells death, extensive Aβ42 release from cells was reported (Friedrich et al., 2009). This study provides insight into how Aβ42 oligomers make their way out of the cell and begin the amyloid cascade.

While the mechanism remains undetermined, this increase in extracellular Aβ42 causes a cytoskeletal protein called Tau to become hyper-phosphorylated and lose its conformation (Asuni et al., 2010; Simic et al., 2016). In healthy cells, tau functions to maintain microtubule structure in axons. How this change in structure occurs is unknown, but a single misfolded and hyper-phosphorylated tau protein results in an increase in the number of tau molecules that are misfolded and hyper-phosphorylated (Asuni et al., 2010; Simic et al., 2016). This theory states that it is tau, not Aβ42, which causes progression of AD. However, Aβ42 remains at the forefront of this theory. Any targets that could prevent aggregation of Aβ42, would be an excellent means of treating AD.

Microglia

With increased levels of Aβ42, either extracellular or intracellular, there are increased levels of pro-inflammatory cytokines. These cytokines are primarily secreted from the resident phagocytic cell of the CNS called microglia. Microglia are myeloid derived cells and share many features with macrophages. Microglia express surface markers like CD11b+, CD45, CD68 and have the capacity to detect and respond to any foreign substance in the CNS. Microglia can assume any of three states: M0 (resting), M1 (inflammatory), M2 (anti-inflammatory). M0 microglia are theoretically ready to shift their activation towards a M1 or M2 state, but recent evidence suggests that M0 microglia may not exist (Tang et al., 2016). Rather, a consistent ratio of M1/M2

microglia is maintained at homeostasis. M1 microglia are activated by lipopolysaccharide (LPS), Aβ42, and other foreign substances. The M1 microglia have a more elongated morphology and secrete cytokines such as: TNF-α, IL-6, and IL-1β. M1 microglia are responsible for recognition of antigens through major histocompatibility complex (MHC) II, processing and generating an inflammatory response by secretion of cytokines and chemokines. Both activities draw other effector cells to the site of inflammation in order to contain and remove antigens in the CNS. Once the antigen has been processed, the inflammatory response must be dampened to prevent consistent inflammation and damage to cells. M2 microglia assume this role by secreting anti-inflammatory cytokines like IL-10. IL-10 reduces inflammation by activating signal transducer and activator of transcription (STAT) 3 (Niemand et al., 2003). STAT3 prevents kinase activity from activating NF-κB (Yu et al., 2009), which prevents NF-κB from acting as a transcription factor for the pro-inflammatory response. IL-10 also inhibits NF-κB mediated inflammation by preventing the MAPK cascade activation and thereby preventing NF-κB from being phosphorylated (Hubo et al., 2013).

Suppressor of Cytokine Signaling 1 and 3

SOCS proteins function to prevent cytokine signaling. Two of the SOCS proteins will be discussed in this review, SOCS1 and SOCS3. Both SOCS proteins function in similar ways to prevent pro-inflammatory cytokine signaling (Yoshimura et al., 2007). SOCS1 can prevent the inflammatory response by preventing kinase activity that would otherwise activate the NF-κB complex. This prevents NF-κB from acting as a transcription factor, and the upregulation of pro-inflammatory cytokines is reduced (Strebovsky et al., 2011). SOCS1 can also interfere with JAK signaling by preventing

phosphorylation of JAK domains. This prevents the activation of the signaling cascade at the beginning and no signal is transduced (Yosimura et al., 2007). SOCS3 inhibits pro-inflammatory cytokine signaling by preventing TRAF6 from activating kinase proteins (Yoshimura et al., 2007). These kinase proteins are no longer active, which prevents activation of NF-κB. A secondary target of SOCS3 suppression of the inflammatory response is IκB which prevents IκB from becoming part of the NF-κB complex. Without the complete molecule, there is no upregulation of pro-inflammatory cytokines through NF-κB (Nair et al., 2011).

SOCS proteins do not only reduce pro-inflammatory cytokines. Both SOCS1 and SOCS3 can reduce the anti-inflammatory cytokine IL-10; both SOCS1 and SOCS3 prevent the phosphorylation, and therefore activation of JAK proteins, to prevent IL-10 mediated signaling (Berlato et al., 2002; Ding et al., 2003). Because IL-10 signaling is autocrine in nature (Saraiva et al., 2010), a strong response by SOCS proteins is required to decrease IL-10 signaling cascades.

Vitamin D3 (VD3

Vitamin D3 (VD3) is a vitamin commonly found in the body and frequently taken as a supplement. VD3 is key for calcium regulation, maintaining healthy teeth and bone structure, and functions as an anti-inflammatory molecule. Importantly, VD3 can cross the blood brain barrier (BBB), so the anti-inflammatory effects are able to take hold in the CNS (Harms et al., 2011). To become an active molecule, VD3 must first undergo two hydroxylation reactions to form the active metabolite 1α, 25-dihydroxyvitamin D3 (1,25-(OH)2VD). This metabolite can enter a cell to bind its receptor, the vitamin d receptor (VDR). Once bound, this ligand/receptor pair moves into the cell and forms a

heterodimer with the retinoid x receptor (RXR). This complex acts as a transcription factor to bind the vitamin d response element (VDRE), leading to upregulation of anti-inflammatory molecules (Wobke et al., 2014; Yin et al., 2014). Furthermore, 1,25-(OH)2D3 can directly prevent transcription of pro-inflammatory molecules in two ways. First, 1,25-(OH)2D3 can enter the cytosol and bind to NF-κB, a transcription factor known to increase the transcription of TNF-α. Second, when the heterodimer of 1,25-(OH)2D3, VDR, and RXR bind to the VDRE, transcription of MAPK phosphatase 1 (MKP1) is increased. MKP1 serves to remove phosphate groups from MAPK signaling molecules, halting the cascade (Wobke et al., 2014); Yin et al., 2014; Boontanrart et al., 2016). VD3 is a powerful modulator of the immune system and should be considered as a means of reducing inflammation in AD (Lue et al., 2010; Lehmann et al., 2011; Boontanrart et al., 2016).

The ratio of M1/M2 microglia is crucial in the progression of AD. The ratio of M1:M2 microglia is increased in AD, as well as the presence of inflammatory cytokines such as TNF-α (Tang et al., 2016). VD3 plays a crucial role in switching microglia activation to a M2 state. Boontanrart et al. (2016) showed that microglia treated with LPS followed with 1,25-(OH)2D3 showed a significant increase in the transcription of IL-10. This secretion of IL-10 would be beneficial in an AD brain, as IL-10 specifically functions to prevent transcription of pro-inflammatory cytokines.

Understanding the Aβ42-related mechanisms of inflammation is crucial to finding a treatment for AD. The amyloid cascade remains the most supported theory but work is still required to verify several components of the theory. Microglia play a large role in the inflammation seen in AD. Their ability to interact with Aβ42 leads to chronic and

damaging inflammation. Future work in studying the effects of not only SOCS proteins but also the anti-inflammatory effects of VD3, would be an important step in determining potential treatments for AD.

Materials and Methods

Cell Lines

Spontaneously Immortalized Microglia (SIM) A9 murine microglia (ATCC, Manassas, VA) were originally derived from cortical tissues collected from 1 day old mice. These microglia are an adherent cell line, and were incubated in 5% CO2 at 37 ºC in a water jacketed incubator. Splitting of this cell line, using a solution of 1 mMEDTA, 1 mM EGTA, and 1 mg/mLGlucose in PBS, occurred 3 to four times a week, and was done at 70% confluency in a T25 or T75 BioLite vented flask with complete growth media. Growth media consisted of 5% Heat Inactivated Horse Serum, 10% Heat Inactivated Calf Serum, and Dulbecco's Modified Eagle Medium (DMEM)-F12. Flasks, serum, and media were purchased from ThermoFisher (Waltham, MA).

Neuro-2a murine neurons (N2A) (ATCC, Manassas, VA) were originally derived from a spontaneous tumor from an albino strain of mouse. Splitting of this cell line using trypsin occurred two to three times a week, and grown in in T25 or T75 BioLite vented flasks in 5% CO2 at 37ºC with complete growth media. Growth media consisted of 5% fetal bovine serum (FBS) in DMEM. DMEM, sera, and dishes were all purchased from ThermoFisher (Waltham, MA).

Cell Counting

Cells were grown to 70% confluency, split from the flask and centrifuged to form a pellet. Cells were re-suspended in 1 mL of complete growth medium. 25 uL of this suspension was mixed with 50 ul of Trypan Blue (Fisher Sciences, Pittsburg, PA), and put onto a hemocytometer. All live cells and all dead cells were counted. For calculating viable cells, the total number of cells in 5 squares, in a total grid of 25, squares were counted. Counting was performed as shown below:

$$\frac{Viable\ Cells}{mL} = \frac{number\ of\ cells\ in\ 5\ squares}{5} * 25\ total\ squares * Dilution\ factor * 10^4$$

$$\frac{Dead\ cells}{mL} = \frac{number\ of\ cells\ in\ 5\ squares}{5} * 25\ total\ squares * Dilution\ factor * 10^4$$

Percent viability was calculated using the following equation:

$$\frac{Viable\ cells}{Viable\ cells + Dead\ Cells} * 100 = \%\ Viability$$

Cell Polarization and Treatments

Microglia were grown to 70% confluency and then treated. To polarize to the M1 state, microglia were treated with LPS (100 ng/mL), IFN-γ (100 ng/mL), and Aβ42 (20 μM). To polarize to the M2 state, microglia were treated with IL-10 (100 ng/mL). Suppressor of Cytokine Signaling (SOCS) 1 and SOCS 3 mimetics were added immediately following treatments at a concentration of 35 μM for each (81 ng/mL and 88 ng/mL respectively). 1,25-(OH)2D3 treatments were initially added at concentrations 1,5,10,15, and 20 ng/mL but these concentrations did not induce IL-10 production by microglia. The concentration of 1,25-(OH)2D3 was increased to 10 μM (42 ng/mL) and 20 μM (84 ng/mL). All treatments were incubated for 24 hours unless noted otherwise.

IFN-γ, IL-10, IL-4 were purchased from BioLegend (San Diego, CA), LPS from *E. coli* 0111.B4 was purchased from Chondrex (Redmond, WA). Vitamin D was purchased from from Sigma Aldrich (ST. Louis, MO). Aβ42 was purchased from rPeptide (Bogard, GA).

ELISA ASSAY

A CorningStar 96 well plate was incubated with capture antibody and incubated overnight. The next day, the capture antibody was aspirated and the plate was washed three times with a wash buffer of PBS and 5% Tween-20. After washing, a standard curve was created in the first two columns. Per manufacturer's directions, the top concentration for the curve was created to be 4000 pg/mL for IL-10 and 1000 pg/mL for TNF-α. From there, a twofold dilution was created for a total of 8 points and duplicated for accuracy. The remaining columns were filled with samples that had been collected and stored at -80°C. After samples were added, the plate was kept at 4°C overnight for maximum detection by the capture antibody. The next day samples and standard curve solutions were aspirated. The plate was again washed three times with wash buffer. Secondary antibody was then added and incubated for 1 hour at room temperature. Wash buffer was then added three times to each well. Avidin-Horseradish Peroxidase (HRP) enzyme was added to each well, and allowed to incubate for 30 minutes at room temperature. Five more wash steps followed, and then substrate was added to each well and allowed to react with enzyme for 15 minutes. A stop solution of 1M phosphoric acid was added to each well to cease any excess color formation. The plate was reader in a SpectraMax Plus 384 Microplate Reader at 450 nm. Each sample was duplicated per plate, and each well was read twice by the reader. If a sample provided a negative optical density (OD) value, and was said to be below the detectable limit, the value was counted

as a zero in this experiment. Data shown are representative of the entire well contents. Triplicates were performed on separate days, and are presented as mean ± SEM. Data were collected using SoftMax Pro 4.8 software. Statistical analysis was performed using an one way analysis of variance (ANOVA) in SigmaPlot 11.0 (Systat Software Inc., San Jose, CA).

Co-Culture Method

Co- culture plates and inserts were purchased from FisherScientific (Waltham, MA). Inserts contained 1 µm size pores in the well to allow for diffusion of microglial cytokines response to the neurons below. In a 24 well plate, 50,000 murine neuronal cells were plated in 700 µL of complete growth media. The insert was then placed into the well, where it sat directly on the top of the neuronal media. 50,000 microglia in 300 µL of complete growth media was added to the insert. The neurons and microglia were incubated in 5% CO2 at 37°C for 24 hours. Following incubation, media for both cell types were aspirated and fresh media added. Treatments were added only to the microglia, and then the cells were incubated in 5% CO2 at 37°C for 24 hours. Following this incubation, inserts containing the microglia were discarded, and the supernatant from the neuronal cells was collected, spun, and stored at -80°C.

To ensure that no microglia projections could fit through the pores of the inserts, crystal violet dye was added to an insert and the inserts were viewed under a parfocal microscope at 400x total magnification. There was no indication of projections coming through the insert by the microglia.

Cytotoxicity Assay

A Lactate Dehydrogenase (LDH) cytotoxicity kit was purchased from Cayman Chemical (Ann Arbor, MI). In a CorningStar 96 well plate, three wells were only plated with neuronal complete growth media. A LDH positive control was plated into the next three wells. For detection of maximum release of LDH by the neurons, 20 µL of Triton X-100 was added. In the last three wells, only cells were plated to determine the spontaneous release of LDH. Cells were added at 50,000 cells per well in 200 µL of complete growth media. These wells were incubated at 37°C for 24 hours. 100 uL of each control well was moved to a fresh 96 well plate, and 100 µL of supernatants from experimental groups were plated. A LDH reaction solution was generated following the manufacturer's instructions. 100 µL of the reaction solution was added to each well, and incubated at 37°C for 30 minutes. The plate was then read for optical density (OD) on the SpectraMax 384 Plus plate reader at 490 nm. To calculate the percent cytotoxicity, the following formula was used:

$$\frac{ExperimentalOD - SpontaneousOD}{MaximumOD - Spontaneous\ OD} * 100 = \%\ Cytotoxicity$$

To ensure that the serum in the complete growth media did not interfere with the results, the OD reading from the media only wells was subtracted from experimental values. Each OD value was converted into a percent cytotoxicity first. Triplicates were performed on separate days, and the data are presented as mean ± SEM. Statistical analysis was done using a one way ANVOA on SigamPlot 11.0 (Systat Software Inc., San Jose, CA).

Immunofluorescence

Eight-chamber slides were purchased from FisherScientific (Waltham, MA). Microgila were seeded into four of the chambers at a density of 5000 cells in 200 µL of media. Neurons were seeded into four of the chambers at a density of 5000 cells in 200 µL of media. Both cell lines were growing on the slide in 5% CO2 at 37 ºC for 24 hours. Following incubation, the media were aspirated and the cells were washed with 1x PBS twice. Cells were fixed using 4% paraformaldehyde and incubated at room temperature for 15 minutes. Following three washes with 1x PBS, both cell lines were permeabilized using 100 µL of 0.2% Triton X100 and incubated at room temperature for 10 minutes. Cells were washed with 1X PBS three times, and then blocked using a blocking solution comprised of 5% goat serum, 3% BSA, 0.5 Tween-20, and 1% BSA. Cells were blocked for 45 minutes at room temperature. The blocking solution was aspirated, and the cells were washed three times with 1X PBS. 50 uL of primary antibody was added to each well at a concentration of 1 mg/mL and incubated at room temperature for 1 hour. Primary antibody was aspirated, and cells were washed three times with 1% BSA. Working in dark conditions, 50 uL of secondary antibody was added at a concentration of 5 µg/mL, and incubated at room temperature for 1 hour. Secondary antibody was aspirated, and the cells were washed with 1% BSA three times. The slide was viewed using an Olympus Epi Fluorescent Spot Scope (Wright State University, Microscope Core). Anti-MAP2 and Goat Anti-Rabbit IgG H&L (Alexa Fluor 488) secondary antibodies were purchased from abcam (Cambridge, MA). Anti-CD 11b and Goat Anti-Rat IgG H&L (Alexa Fluor 488) were purchased from abcam (Cambridge, MA).

IMMUNOFLUORESENCE SLIDE SETUP

N2A • 1°: MAP2 • 2°: Goat Anti-Rabbit IgG H&L (Alexa Fluor 488)	N2A • 1°: CD 11b • 2°: Goat Anti-Rat IgG H&L (Alexa Fluor 488)	SIM-A9 • 1°: MAP2 • 2°: Goat Anti-Rabbit IgG H&L (Alexa Fluor 488)	SIM-A9 • 1°: CD 11b • 2°: Goat Anti-Rat IgG H&L (Alexa Fluor 488)
SIM-A9 • 1°: MAP2 • 2°: Goat Anti-Rabbit IgG H&L (Alexa Fluor 488)	SIM-A9 • 1°: CD 11b • 2°: Goat Anti-Rat IgG H&L (Alexa Fluor 488)	N2A • 1°: MAP2 • 2°: Goat Anti-Rabbit IgG H&L (Alexa Fluor 488)	N2A • 1°: CD 11b • 2°: Goat Anti-Rat IgG H&L (Alexa Fluor 488)

Results

1,25-(OH)2D3 induces Microglia to Secrete IL-10, but Requires SOCS mimetics to Reduce TNF-α Production in the Presence of LPS and/or IFN-γ

To determine what concentration of 1,25-(OH)2D3 would stimulate IL-10 secretion from microglia, concentrations of 1,5,10,15, or 20 ng/mL of 1,25-(OH)2D3 were incubated with the microglia for 6,12,18, and 24 hours. None of these concentrations or time points resulted in any production of IL-10 (data not shown). Concentrations of 10 µM (42 ng/mL) and 20 µM (84 ng/mL) were used instead, and were also treated with LPS alone, or LPS+IFN-γ. This combination of treatments resulted in IL-10 production as measured by ELISA (Figure 5). However, only the 20 µM concentration of 1,25-(OH)2D3 resulted in significant increases in IL-10 as compared to a negative control ($p<0.05$) (Fig. 6; Table 1). Both SOCS1 mimetic and SOCS3 mimetic reduced IL-10 concentrations to below the detectable range of the assay, regardless of the treatment group (data not shown).

TNF-α production by microglia was also measured by ELISA. Addition of 1,25-(OH)2D3 to LPS, IFN-γ or LPS+IFN-γ groups did not result in any significant reduction in TNF-α production (Figure 7; Table 2). However, treatment with SOCS1 mimetic, SOCS3 mimetic or SOCS1 mimetic with SOCS3 mimetic significantly reduced TNF-α production even further ($p<0.05$) (Figure 7; Table 2). When 1,25-(OH)2VD was added

along with SOCS mimetics to LPS and IFN-γ treatments, TNF-α production was reduced even further ($p<0.05$) (Figure 7; Table 2).

Microglia treated with Aβ42 secrete TNF-α, which can be reduced by 1,25-(OH)2D3 and SOCS-Mimetics

To determine the M1 stimulation properties of Aβ42, microglia were seeded with 20 μM Aβ42. Using an ELISA, it was determined that microglia do secrete TNF-α in the presence of Aβ42 (Figure 8; Table 3). 1,25-(OH)2D3 was added to Aβ42 treatments, along with SOCS mimetics, to determine if the production of TNF-α by Aβ42 could be reduced. 1,25-(OH)2D3 can reduce the production of Aβ42 ($p<0.05$) to nearly half of the Aβ42 treatment alone (Figure 8; Table 3). The secretion of TNF-α was also reduced by the addition of both SOCS1 and SOCS3 mimetics ($p<0.05$) (Figure 8; Table 3).

In the presence of Aβ42, 1,25-(OH)2D3 does not stimulate IL-10 secretion

Microglia were treated with 20 μM Aβ42, and then treated with 1,25-(OH)2D3 and/or SOCS proteins. Only SOCS1 and SOCS1+1,25-(OH)2D3 induced IL-10 secretion, but neither was statistically significant (Figure 9; Table 4).

In a Co-Culture of Neurons and Microglia, Aβ42 induces TNF-α secretion, but 1,25-(OH)2D3 and SOCS mimetics reduce TNF-α concentrations

Aβ42 induced TNF-α secretion which was detectable in neuronal supernatant. TNF-α secretion was significantly reduced by 1,25-(OH)2D3 and SOCS mimetics ($p<0.05$) (Figure 10; Table 5). 1,25-(OH)2D3 significantly reduced TNF-α secretion following Aβ42 treatment ($p<0.05$) (Figure 10; Table 5). The combination of SOCS1 mimetic and SOCS3 mimetic reduced TNF-α levels to near zero ($p<0.05$) (Figure 10;

Table 5). 1,25-(OH)2D3 and SOCS mimetics in concert reduced TNF-α concentrations to near zero values ($p<0.05$) (Figure 10; Table 5).

In a Co-Culture of Neurons and Microglia, Aβ42 does not induce IL-10 secretion

No significant secretion of IL-10 was detected following 20 μM of Aβ42 (data not shown).

Immunofluorescence staining of SIM-A9 and N2A cells

SIM-A9 microglia and N2A neurons were each stained with anti-CD11b+ and anti-MAP2 antibodies for immunofluorescent confirmation of each cell lines identity. As expected, microglia expressed CD11b+ and neurons did not (Figure 11). Neurons expressed MAP2 and microglia did not (Figure 11).

Cell Viability and Cell Cytotoxicity Assays

Using trypan blue exclusion dye, neuronal cells from co-culture plates were stained for viability. Compared to untreated cells, all treatment groups had approximately a 1.5-fold decrease in viability ($p<0.05$) (Figure 12). To supplement these data, a cytotoxicity assay was performed. Aβ42 treated cells showed little cytotoxicity, while 1,25-(OH)2D3 treated cells, compared to those treatments without 1,25-(OH)2D3, showed approximately a 1.5-fold increase in cytotoxicity ($p<0.05$) (Figure 13).

Discussion

Aβ42 has been associated with the pathology of AD since its discovery (Glenner and Wong, 1984), but its role has not yet been determined. The amyloid cascade theory suggests that Aβ42 aggregation begins an inflammatory-related cascade that leads to tau hyper-phosphorylation and, therefore, resulting in AD. However, how Aβ42 aggregates start the cascade remains unknown. Several studies have identified the inflammatory response as the mechanism behind the cascade. Understanding the inflammatory response to Aβ42, and its effects on neurons, would prove useful to better understanding AD pathogenesis.

Vitamin D3 (VD3) is a known anti-inflammatory substance (Yin et al., 2014). Physiological levels of VD3 have been reported anywhere from 20 ng/mL to 100 ng/mL (Holick, 2009). Our study used a concentration of 84 ng/mL, well within this range. The active form of VD3, 1,25-(OH)2D3, can bind its cytosolic receptor, the vitamin D receptor (VDR). Once 1,25-(OH)2D3 binds the VDR, the retinoid X receptor (RXR) binds the 1,25-(OH)2D3 and VDR complex to form a heterodimer (Kongsbak et al., 2013). This heterodimer can then act as a transcription factor to upregulate transcription of IL-10 and MAP kinase phosphatase 1(Wobke et al., 2014; Yin et al., 2014). In this experiment, 1,25-(OH)2D3 alone could not induce IL-10 secretion. Microglia required a M1 stimulant to allow for transcription of IL-10. Microglia treated with LPS, followed

by 1,25-(OH)2D3, do secrete IL-10 through MAPK signaling, where VDR transcription is upregulated as a protective measure to the inflammatory response (Wobke et al., 2014). Following LPS treatment, VDR is more highly expressed (Boontanrart et al., 2016), and therefore more available to bind 1,25-(OH)2D3. As a result, IL-10 is more prevalent in supernatant.

Based on previous literature, TNF-α concentrations were expected to decrease after the addition of 1,25-(OH)2D3 (Boontanrart et al., 2016). Boontanrart et al. (2016) showed that transcription of pro-inflammatory cytokines decreases in the presence of 1,25-(OH)2D3, while the transcription of anti-inflammatory cytokines increased. In this experiment, 1,25-(OH)2D3 did not reduce TNF-α production following LPS treatment, nor did IL-10 production increase. This result could be a limitation of studying inflammation in our study in that an *in vitro* study cannot have all of the immune system interactions that would occur *in vivo*. The same study was able to show IL-10 increases in the presence of a M1 stimulant such as LPS, but only transcription was measured by real time PCR, no functional data based on these transcripts was provided (Boontanrart et al., 2016). It could be that transcription does not correlate to expression of IL-10, where post transcriptional modifications may be masking the effects of IL-10.

However, the addition of SOCS mimetics did reduce TNF-α, as well as IL-10 production. This was an expected result, as SOCS1 mimetics and SOCS3 mimetics are both known to reduce cytokine production (Ahmed et al., 2015; Reichard et al., 2010). When 1,25-(OH)2D3 was added along with SOCS mimetics, TNF-α production was reduced even further. The combinatory anti-inflammatory effects of 1,25-(OH)2VD and SOCS mimetics suggests that SOCS mimetics suppression of TNF-α secretion allows for

the anti-inflammatory effect of 1,25-(OH)2D3 to take hold. This result occurs even when microglia are treated with LPS and IFN-γ, both of which are strong inducers of inflammation. With the addition of SOCS1 and SOCS3 together, followed by 1,25-(OH)2D3, there was no TNF-α secretion following LPS and IFN-γ treatment. The lack of TNF-α suggests that the ratio of SOCS1:3 activation plays an important role in modulating not only the pro-inflammatory response, but allowing the anti-inflammatory effects of 1,25-(OH)2D3 to play a more crucial role in reducing inflammation. Reichard et al. (2010) studied the ratio of SOCS1:SOCS3 expression *in vitro* by flow cytometry analysis. M1 stimulated cells showed an increase in SOCS1 expression, while M2 stimulated cells showed an increase in SOCS3 (Reichard et al., 2010). However, cytokine response was not measured in this experiment. This current experiment showed that upregulation of either SOCS1 or SOCS3 using the SOCS mimetics decreases both the pro-inflammatory and anti-inflammatory responses while demonstrating that SOCS mimetic proteins and 1,25-(OH)2VD work together to reduce Aβ42 related inflammation. A separate study with complete knockout out SOCS1 and SOCS3 in mice found a significant increase in the secretion of TNF-α in their knockout mice (Ushiki et al., 2016). This increase in TNF-α was also directly correlated with an increase in cell death and an overall increase in inflammatory disease (Ushiki et al., 2016).

While the SOCS mimetics were effective at reducing TNF-α concentrations, IL-10 was also impacted by these mimetics. The lack of IL-10 would be a harmful effect *in vivo*, as demonstrated by Ko et al. (2012). This group found that IL-10 knockout mice showed a decrease in percent survival and an increase in inflammatory cytokines. Clearly, IL-10 is a necessary cytokine and reducing IL-10 concentrations with SOCS

mimetics is a limitation of this study where we showed SOCS mimetics decreased IL-10 to below detectable ranges of the ELISA assay. But, further study would be required to determine if this same effect occurs *in vivo*.

In these co-culture experiments, Aβ42 was shown to induce TNF-α secretion by microglia into neuronal supernatant. It was anticipated that TNF-α would result in an increase in neuronal death. However, 75% of neurons stained viable using trypan blue dye. This was substantiated using a LDH cytotoxicity assay that showed minimal cytotoxicity in neurons from co-cultures where microglia were treated with Aβ42. Aβ42 has previously been shown to not induce neuronal apoptosis (Carter et al., 2001), and these results confirm this. Interestingly, the cytotoxicity of 1,25-(OH)2D3 treated co-cultures was significantly increased compared to treatment groups lacking 1,25-(OH)2D3. Weitsman et al. (2003) showed that VD3 increased cytotoxicity of human breast cancer cells. Using Western blotting, this group showed that caspase activity increased with concentration of calcitriol and time of exposure. These findings substantiate our findings and suggest a detrimental role of 1,25-(OH)2D3. Previous work has shown that 1,25-(OH)2D3 increases reactive oxygen species (ROS) concentrations (Koren et al., 2000; Weitsman et al., 2003). The increase in cytotoxicity may be related to an increase in ROS. More work is required to determine the exact cause of this cytotoxicity.

A future *in vitro* experiment would use primary microglia and primary neurons from rats as opposed to the cell lines that were used in the current study. In addition to seeding microglia with Aβ42, tau monomers, tau oligomers, and hyper-phosphorylated tau oligomers would all be added to microglia in separate experiments. This new study

would aim to better understand the amyloid cascade along with investigating the inflammatory response to both Aβ42 and tau. Importantly, the ratios of SOCS1 and SOCS3 would be monitored at 6, 12, 18, and 24 hours with cytokine response measured by ELISA at the same time points. These results would add to the understanding of AD as an inflammatory disease, while also attempting to better understand the initial processes that lead to AD pathology.

Future Studies

Using a rat model, the anti-inflammatory effects of 1,25-(OH)2D3 could be tested in an AD-like model. This model would aim to study neuroinflammation, and to investigate the amyloid cascade theory. In individual experiments, a guided CRISPR-Cas9 system would be developed to remove the wildtype genes for BACE1, ApoE, and γ-secretase. The CRISPR-Cas9 system would utilize donor templates for each listed gene, where one allele is knocked out. To test the effects of the CRISPR-Cas9 system, edits with no donor templates would need to be run first, to determine if the rats would survive the gene editing. A similar model was performed by Paquet et al. (2016), where CRISPR was used to generate APP knockout neurons which either had a single mutated allele or complete knockout of the APP gene. A CRIPSR system is available for purchase from Origene for each gene. (Rockville, MD), but this technique would need to be optimized as little work has been done with these CRISPR models. Each gene group would contain 10 rats, and each group would receive a single CRISPR-Cas9 treatment to provide mutated forms of either BACE1, ApoE, or γ-secretase. Western blots would be performed to determine the presence of each mutated protein. Following CRISPR editing and gene addition, rats would be monitored for three separate time points: 1,2, and 3 months (n=3 rats per time point). Rats will have weekly behavior checks (using the Radial Arm Water Maze (RAWM) technique) (Puzzo et al., 2014) to determine if the mutated gene is reducing their cognitive abilities. The RAWM apparatus has six arms, each of which lead to the center of the device. A rat is placed at the end of an arm, and

can search for a food item in an open area. One week later, the same rat will enter the same arm of the device, but the food item is moved behind a sliding hinge door, while a new door is opened. The goal is for the rat to acknowledge spatial cues and use working memory to determine where the food item last was. If the rat has a good working memory, it should be able to reach the food item. CRISPR-Cas9 edited rats for ApoE would be expected to perform more poorly than those with mutated BACE1 or γ-secretase. After their assigned time point has ended, rats would be sacrificed by decapitation. The brain would be collected, along with blood (peripheral and brain), and cerebrospinal fluid (CSF). Cytokines from blood and CSF would be tested for the presence of M1 and M2 cytokines by ELISA. Blood and CSF would also be tested for Aβ40 and Aβ42 by ELISA. Brain tissue would be prepared for immunohistochemical analysis of apoptotic markers. More brain tissue would be used for isolation of microglia. Using Western blots, the ratio of SOCS1/SOCS3 would be determined from primary microglia collected from control and experimental rats for each monthly time point following the sacrifice of the rat. Once bioassays and analysis have been completed from these animals, the same treatment groups and number of rats would be treated with the addition of 1,25-(OH)2D3 to experimental rat groups. A control group would have only 1,25-(OH)2D3 treatment but with CRISPR editing or gene addition. Separate groups of rats would receive a daily dose of 1,25-(OH)2D3 for their allotted experimental time point. The range of 1,25-(OH)2VD treatments would be 10 µM, 20 µM, 30 µM, 40 µM, and 50 µM. Groups of three rats would receive a specific concentration of 1,25-(OH)2VD for their specific monthly time point. These rats would then be sacrificed, and the same assays would be run. The range of 1,25-(OH)2VD treatments would provide

more insight into which concentrations of 1,25-(OH)2VD are toxic and which are beneficial.

The goal of this study would be to observe not only the inflammatory response to common AD mutations, but to determine the role that SOCS protein ratios play in controlling the inflammation within the CNS. We predict that this experiment would show three points: mutated BACE1 decreases Aβ42 concentrations in CSF and blood, mutated ApoE increases Aβ42 concentrations in CSF and blood, and mutated γ-secretase decreases Aβ42 concentrations. If these predications were supported, these data would suggest that the amyloid cascade theory is the correct approach to understanding AD. However, if these predictions do not work out as expected, then these data would suggest that the splicing of the APP does not play a large role in AD pathology, and that ApoE mutations do not impact the formation of Aβ aggregates.

Figures

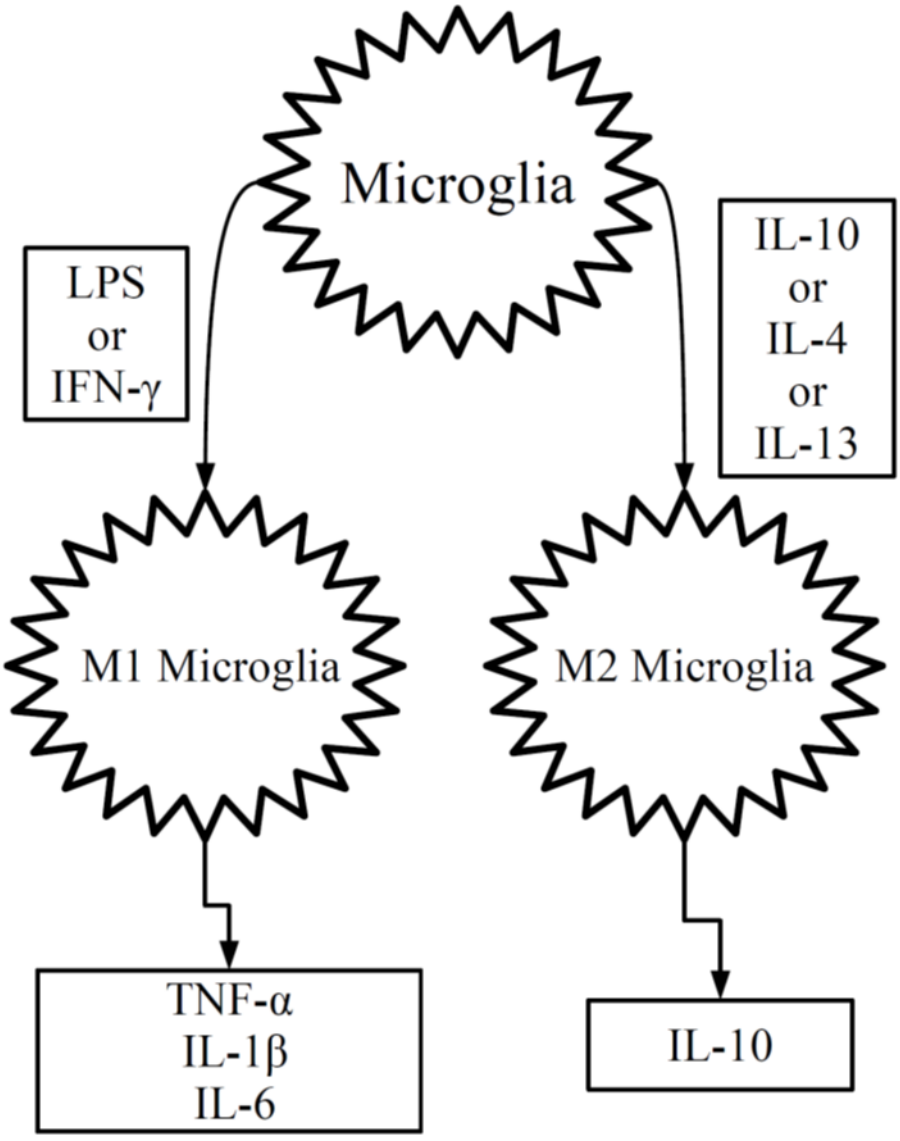

Figure 1. Mechanism of microglial activation into M1 and M2 states (As adapted from Yin et al., 2014)

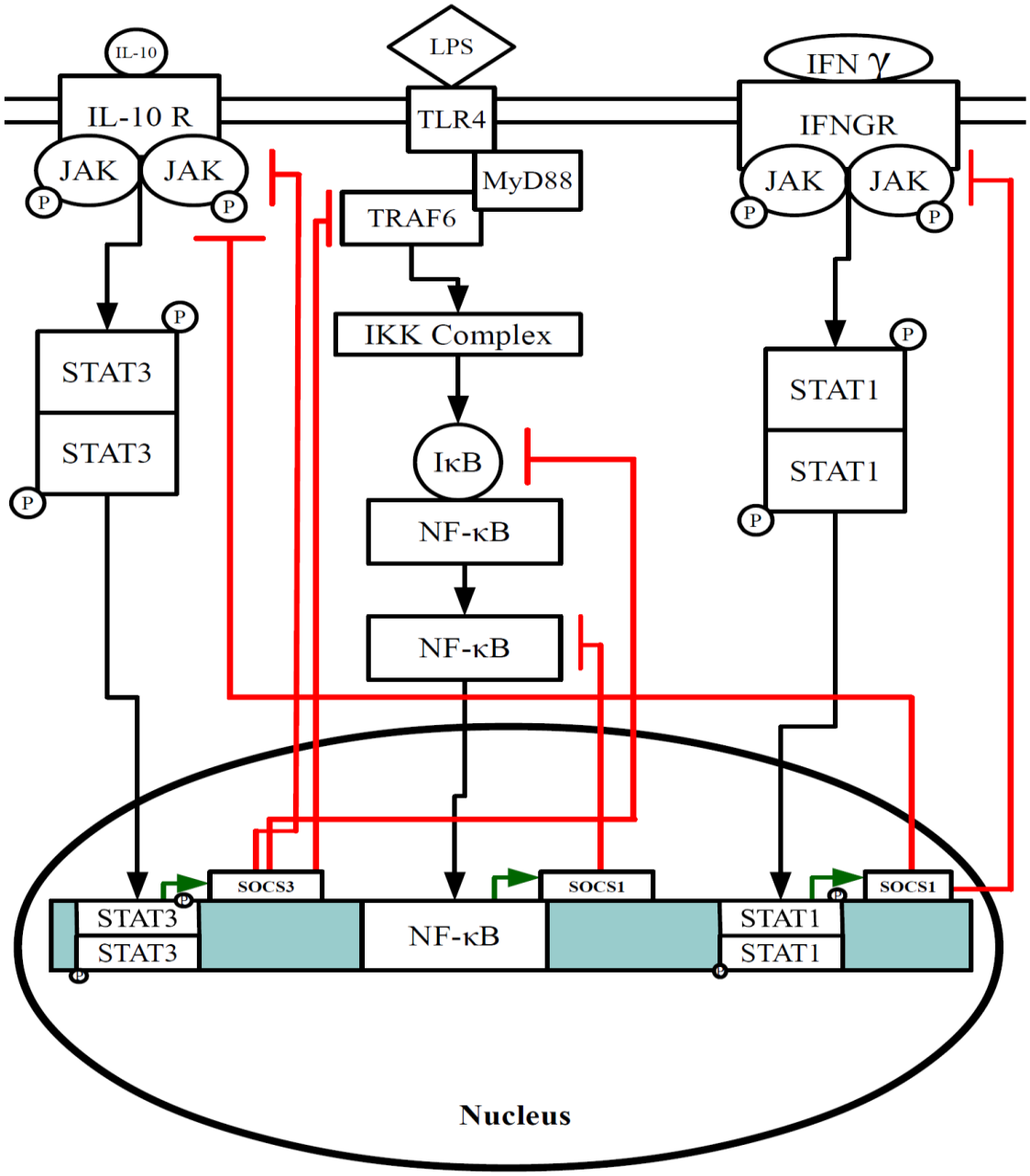

Figure 2. Proposed mechanism: Inhibition of pro- and anti-inflammatory pathways by SOCS1 and SOCS3. IL-10 binds its receptor which leads to phosphorylation of JAK domains. JAK phosphorylates STAT3, that then acts as a transcription factor to upregulate the expression of SOCS3. LPS binds TLR4, which activates the NF-κB signaling cascade. NF-κB acts as a transcription factor to upregulate the expression of SOCS1. IFN-γ binds its receptor, phosphorylating JAK domains. JAK phosphorylates STAT1, which acts as a transcription factor to upregulate expression of SOCS1. SOCS3 can inhibit IL-10 signaling by binding JAK domains directly. SOCS3 can bind IκB which prevents the assembly of IκB into the NF-κB complex, preventing NF-κB from upregulating pro-inflammatory cytokines. If the NF-κB complex is formed, SOCS3 can bind the complex directly to prevent NF-κB from acting as a transcription factor and therefore preventing pro-inflammatory cytokines from being transcribed. SOCS1 also binds NF-κB, which prevents transcription of pro-inflammatory cytokines. SOCS1 binds to JAK domains, both on the IL-10 receptor and IFN-γ receptor, preventing transcription of both pro-inflammatory and anti-inflammatory cytokines. (As adapted from Neimand et al., 2007; Strebovsky et al., 2011; Yin et al., 2014)

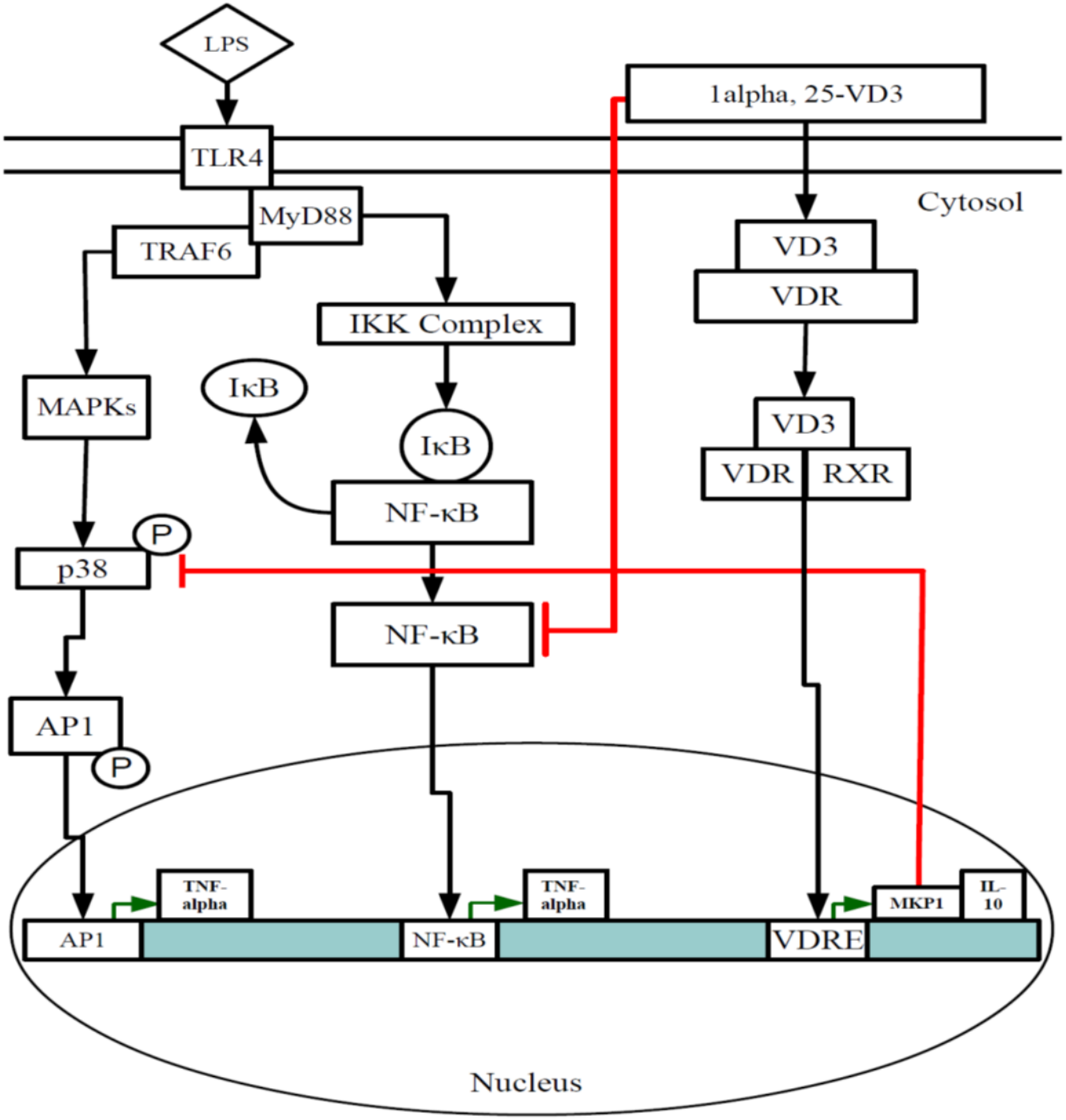

Figure 3. Proposed mechanism: 1,25-(OH)2VD Induced IL-10 Secretion and Reduction of TNF-α Following LPS Treatment. Following LPS stimulation, Microglia secrete TNF-α through two pathways: MAPK signaling and NF-κB signaling. 1,25-(OH)2VD has the ability to reduce this secretion of TNF-α by directly binding to the NF-κB complex to prevents the transcription of TNF-α. 1,25-(OH)2VD can also bind the VDR and RXR to form a complex capable of binding to the VDRE. Transcription of MKP1 (MAPK phosphatase1) and IL-10 are upregulated as result of the VDRE being bound by the 1,25-(OH)2VD, VDR, and RXR complex. MKP1 dephosphorylates p38, which ends the MAPK signaling cascade and prevents TNF-α expression. (As adapted from Wobke et al., 2014 and Yin et al., 2014)

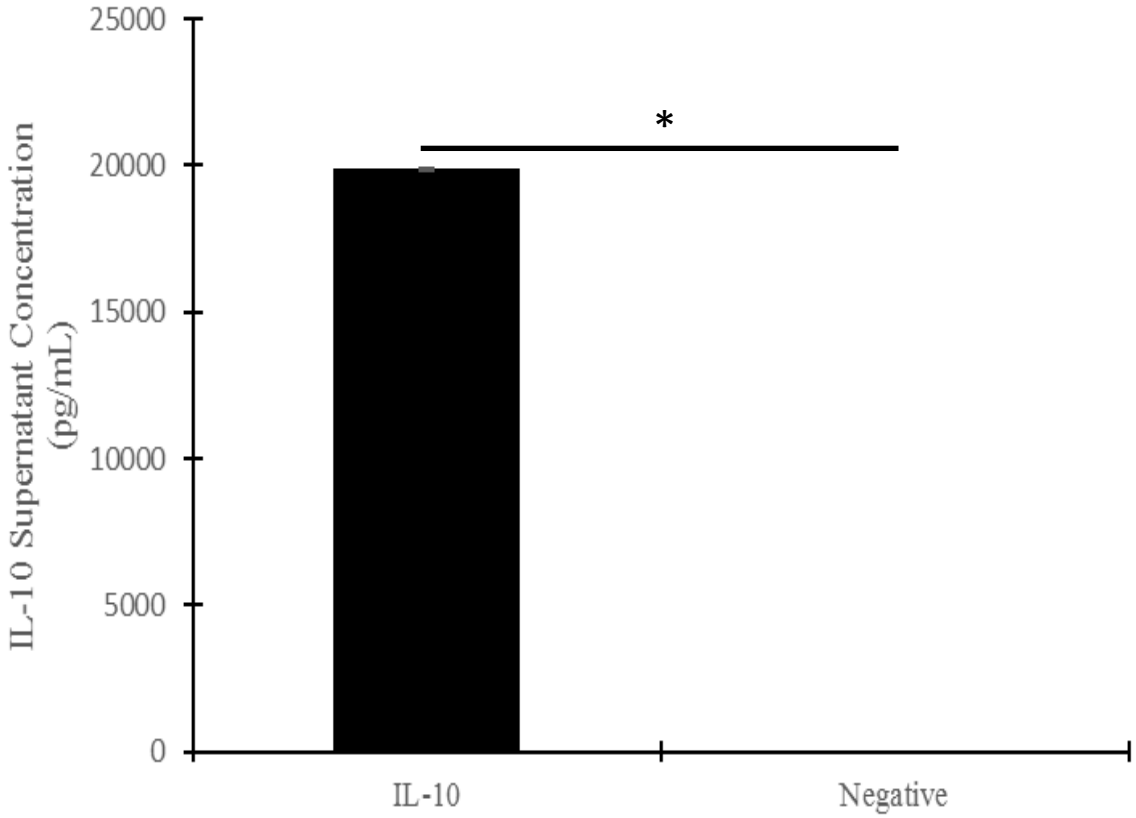

Figure 4. IL-10 positive control for ELISA. Microglia were treated with IL-10 (100 ng/mL). After 24 hours of incubation, supernatant was collected and put onto a coated anti-IL-10 ELISA plate. The amount of IL-10 added was subtracted from the total concentration of IL-10 to give the true supernatant concentration of IL-10. Significance (*) was determined using an ANOVA ($p<0.05$). The graph represents three individual repeated experiments.

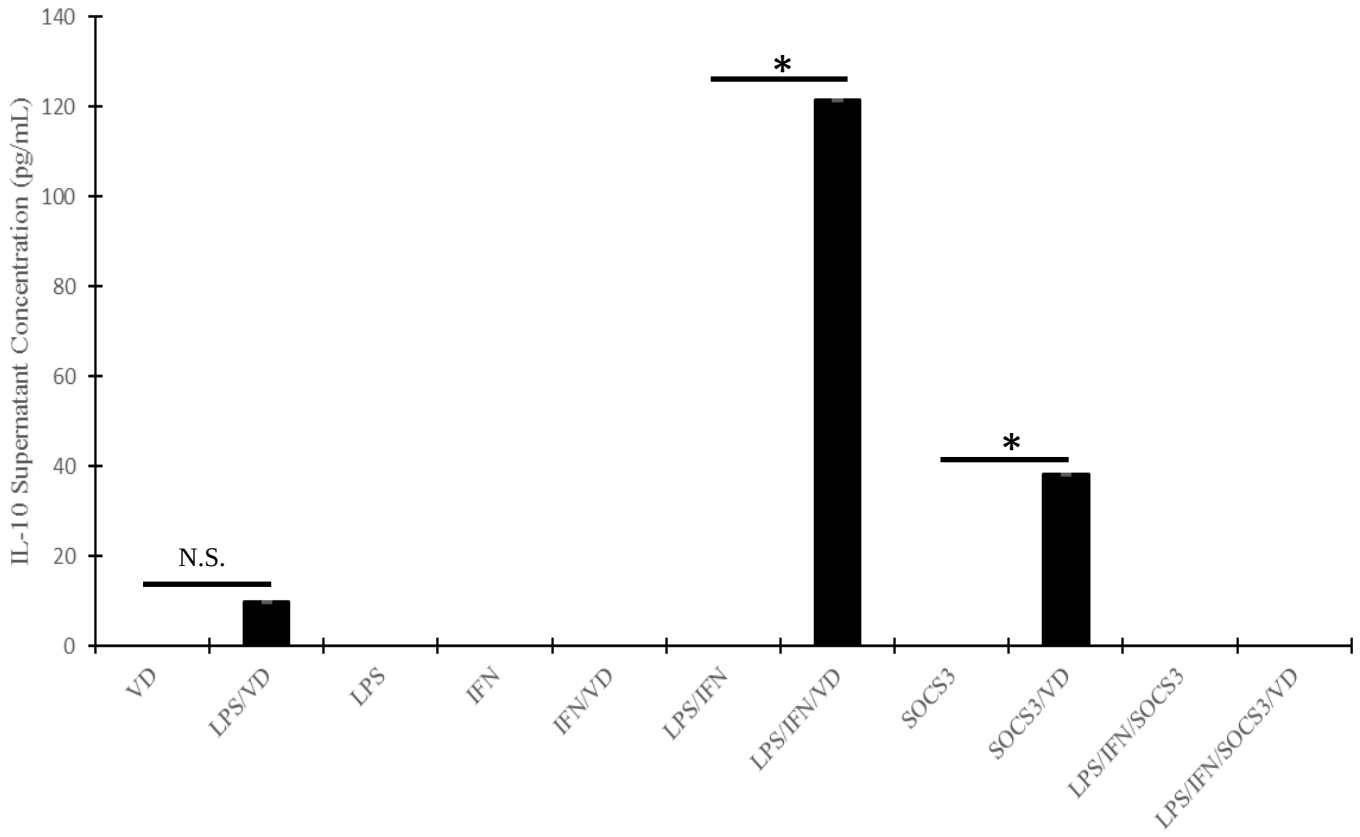

Figure 5. Microglia secretion of IL-10 is not induced by 10 μM 1,25-(OH)2VD after LPS treatment. SIM-A9 microglia were treated with LPS (100 ng/mL), IFN-γ (100 ng/mL), SOCS3 mimetic (35 μM), and 1,25-(OH)2VD (10 μM). After 24 hours of incubation, supernatant was collected and put onto a coated anti-IL10 ELISA plate. The addition of SOCS mimetics reduced IL-10 secretion below the detectable range of the assay (32 pg/mL). All significance (*) was determined using an ANOVA ($p<0.05$). This graph represents three individual repeated experiments.

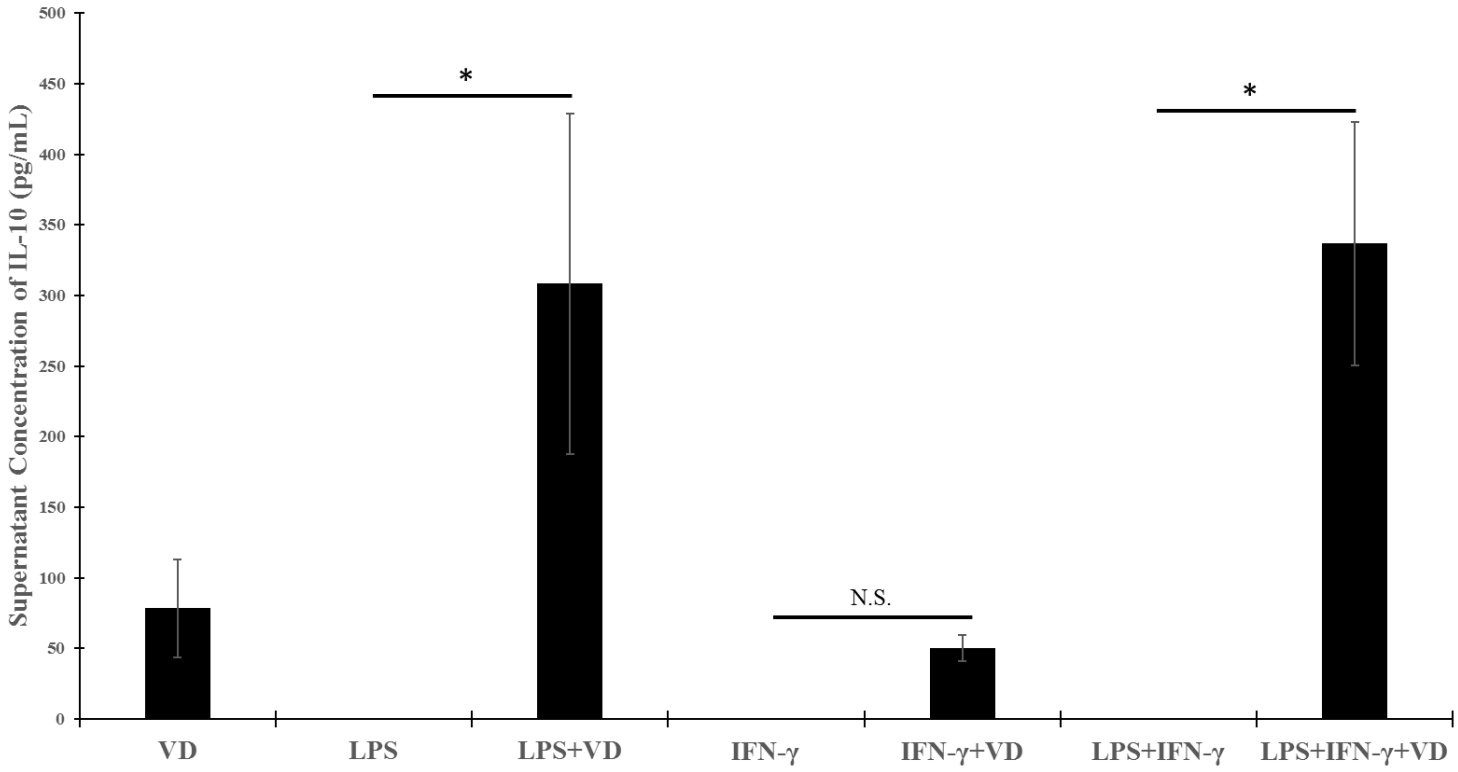

Figure 6. Microglia secretion of IL-10 is induced by 20 µM 1,25-(OH)2VD only after LPS treatment. SIM-A9 microglia were treated with LPS (100 ng/mL), IFN-γ (100 ng/mL), SOCS1 mimetic (35 µM), SOCS3 mimetic (35 µM), and VD (20 µM). After 24 hours of incubation, supernatant was collected and put onto a coated anti-IL10 ELISA plate. The addition of SOCS mimetics reduced IL-10 secretion below the detectable range of the assay (32 pg/mL; Data not shown). All significance (*) was determined using an ANOVA ($p<0.05$). This graph represents three individual repeated experiments.

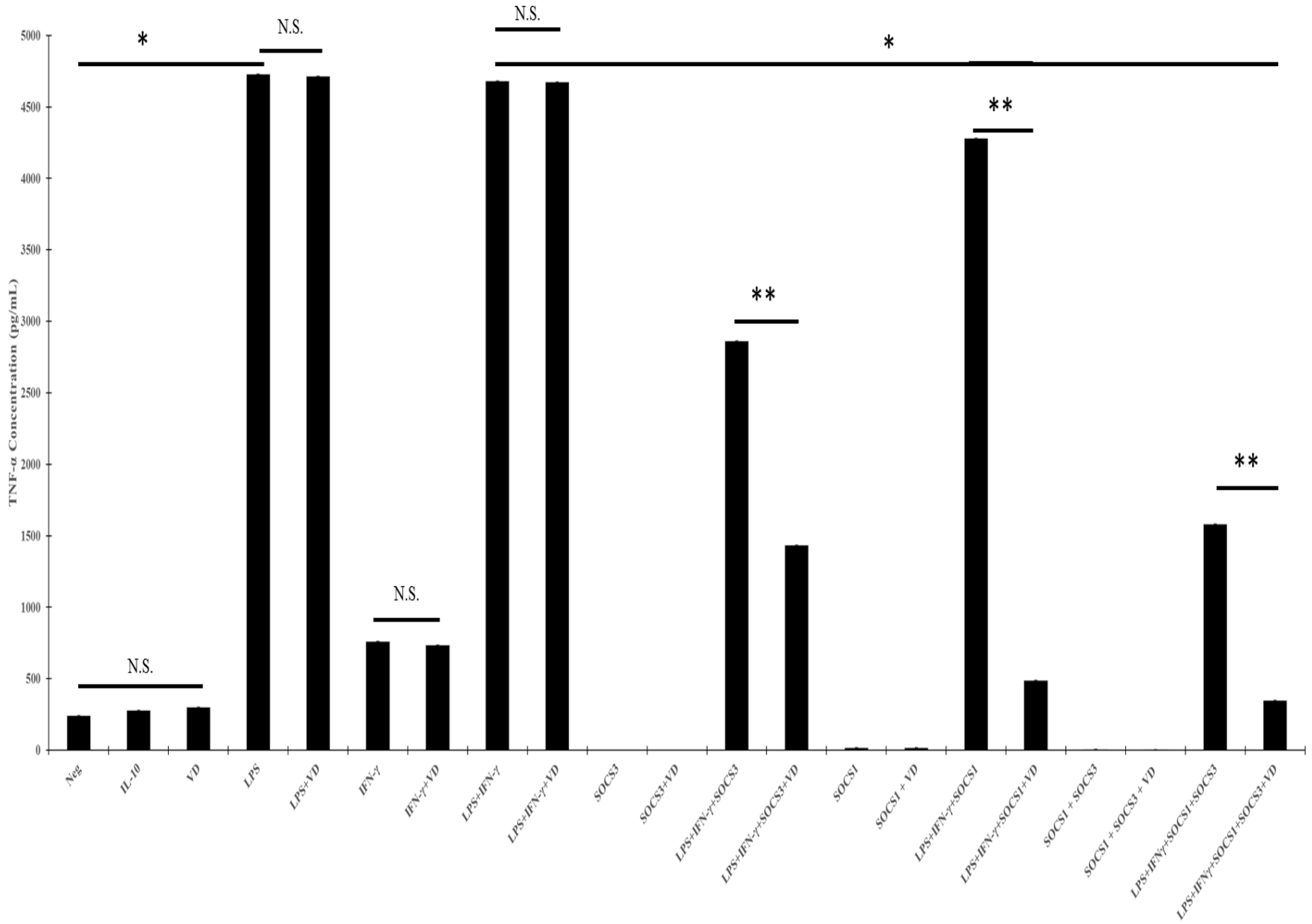

Figure 7. Microglia secretion of TNF-α is reduced by the combination of 1,25-(OH)2VD and SOCS mimetics. SIM-A9 microglia were treated with LPS (100 ng/mL), IFN-γ (100 ng/mL), SOCS1 mimetic (88 ng/mL), SOCS1 mimetic (35 μM), SOCS3 mimetic (35 μM), and VD (20 μM). After 24 hours of incubation, supernatant was collected and put onto a coated anti-TNF-α ELISA plate. The addition of both 1,25-(OH)2VD and SOCS protein mimetic significantly reduces the concentration of TNF-α in microglia supernatant. All significance (* and ** compared to VD treatment group) was determined using an ANOVA ($p<0.05$). This graph represents three individual repeated experiments.

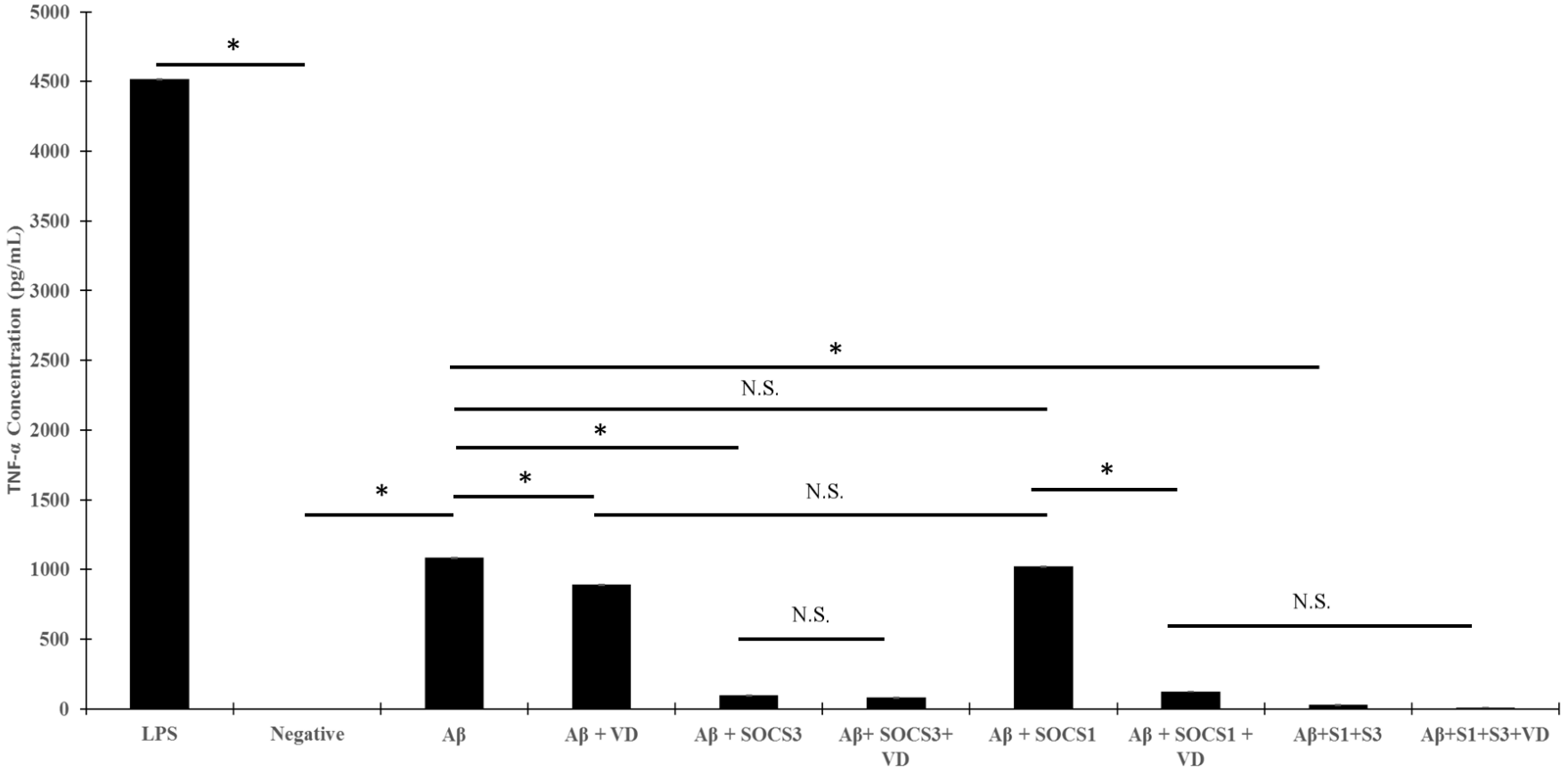

Figure 8. Aβ42 induces secretion of TNF-α by microglia, but is reduced in the presence of 1,25-(OH)2VD and SOCS mimetics. Microglia were treated with LPS (100 mg/mL), Aβ42 (20 μM), SOCS1 mimetic (35 μM), SOCS3 mimetic (35 μM), and 1,25-(OH)2VD (20 μM). After 24 hours of incubation, microglia supernatant was collected and put onto a coated anti-TNF-α ELISA plate. 1,25-(OH)2VD significantly reduced the concentration of TNF-α as compared to Aβ42 treatment alone. While SOCS1 mimetic treatment alone did not reduce TNF-α concentrations, while SOCS3 mimetic and SOCS1 mimetic were both effective at reducing TNF-α concentrations. Except for SOCS3 mimetic treatment, the addition of 1,25-(OH)2VD to the SOCS mimetic treatments reduced TNF-α concentrations even closer to zero values. All significance (*) was determined using an ANOVA (N.S.- not significant). The graph represents three individual repeated experiments.

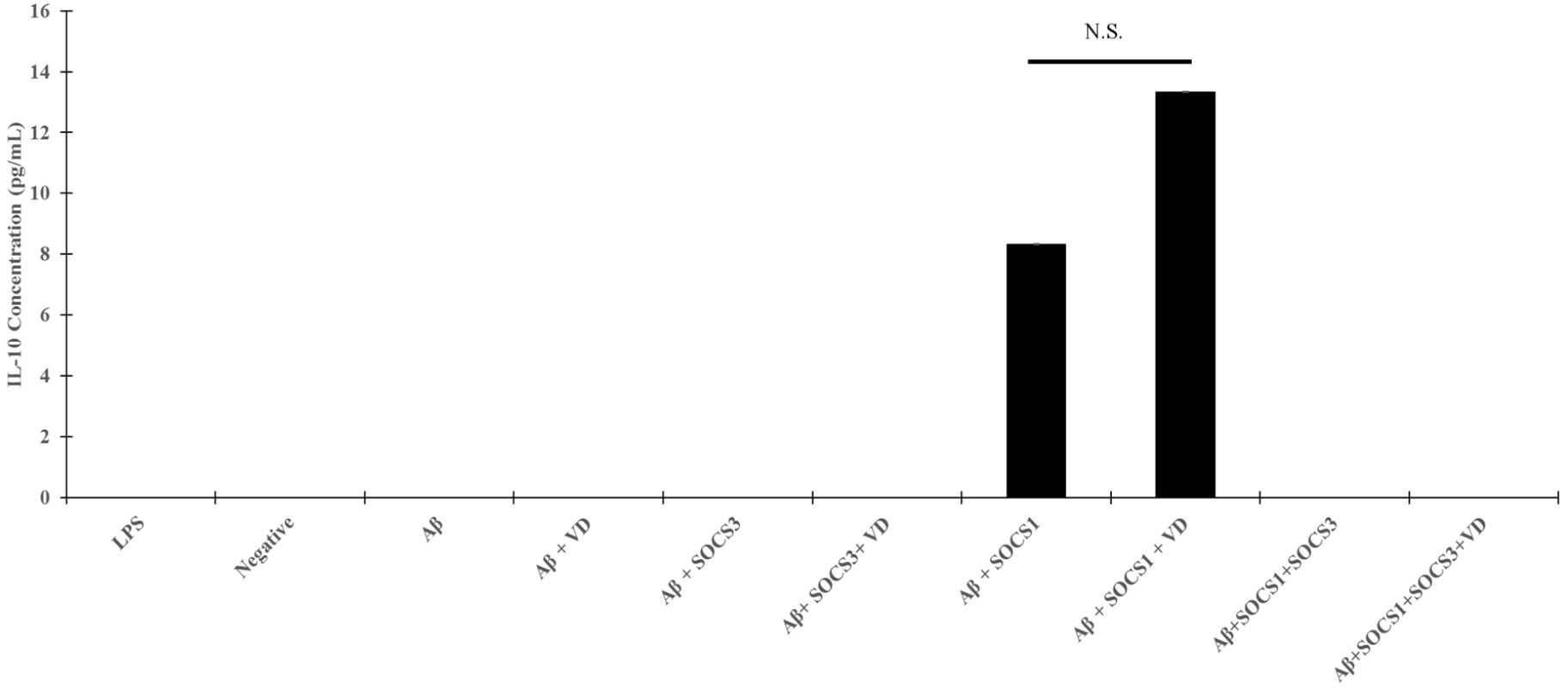

Figure 9. Aβ42 does not induce secretion of IL-10 by microglia. Microglia were treated with LPS (100 mg/mL), Aβ42 (20 μM), SOCS1 mimetic (35 μM), SOCS3 mimetic (35 μM), and 1,25-(OH)2VD (20 μM). After 24 hours of incubation, microglia supernatant was collected and put onto a coated anti-IL-10 ELISA plate. 1,25-(OH)2VD did not induce IL-10 secretion into microglia supernatant. SOCS1 mimetic along with 1,25-(OH)2VD did induce IL-10 but these concentrations were not statistically significant (N.S.- not significant). The graph represents three individual repeated experiments.

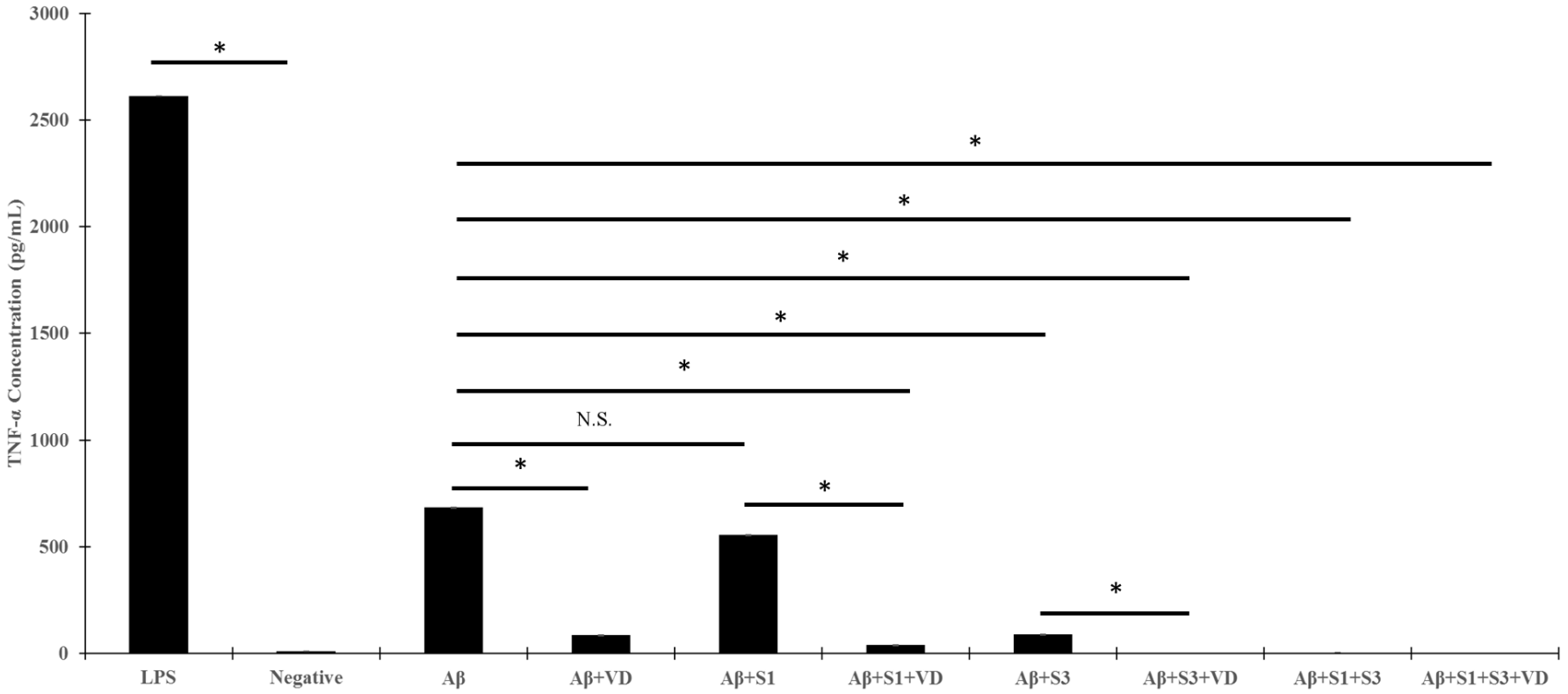

Figure 10. 1,25-(OH)VD and SOCS mimetics are able to reduce TNF-α concentrations in neuronal supernatant from an AD-like co-culture model following treatment with Aβ42. Microglia were treated with LPS (100 mg/mL), Aβ42 (20 μM), SOCS1 mimetic (35 μM), SOCS3 mimetic (35 μM), and 1,25-(OH)2VD (20 μM). After 24 hours of incubation, microglia supernatant was collected and put onto a coated anti-TNF-α ELISA plate. In a co-culture model of microglia and neurons, 1,25-(OH)2VD was able to significantly reduce the concentration of TNF-α. While SOCS1 mimetic alone was not able to achieve the same result, addition of 1,25-(OH)2VD to SOCS1 mimetic significantly reduce the concentration of TNF-α. SOCS3 mimetic, along with the combination of both SOCS1 mimetic and SOCS3 mimetic were successful in reducing TNF-α concentrations, and this effect was exacerbated by the addition of 1,25-(OH)2VD. All significance (*) was performed using an ANOVA (N.S.- not significant). The graph represents three individual repeated experiments.

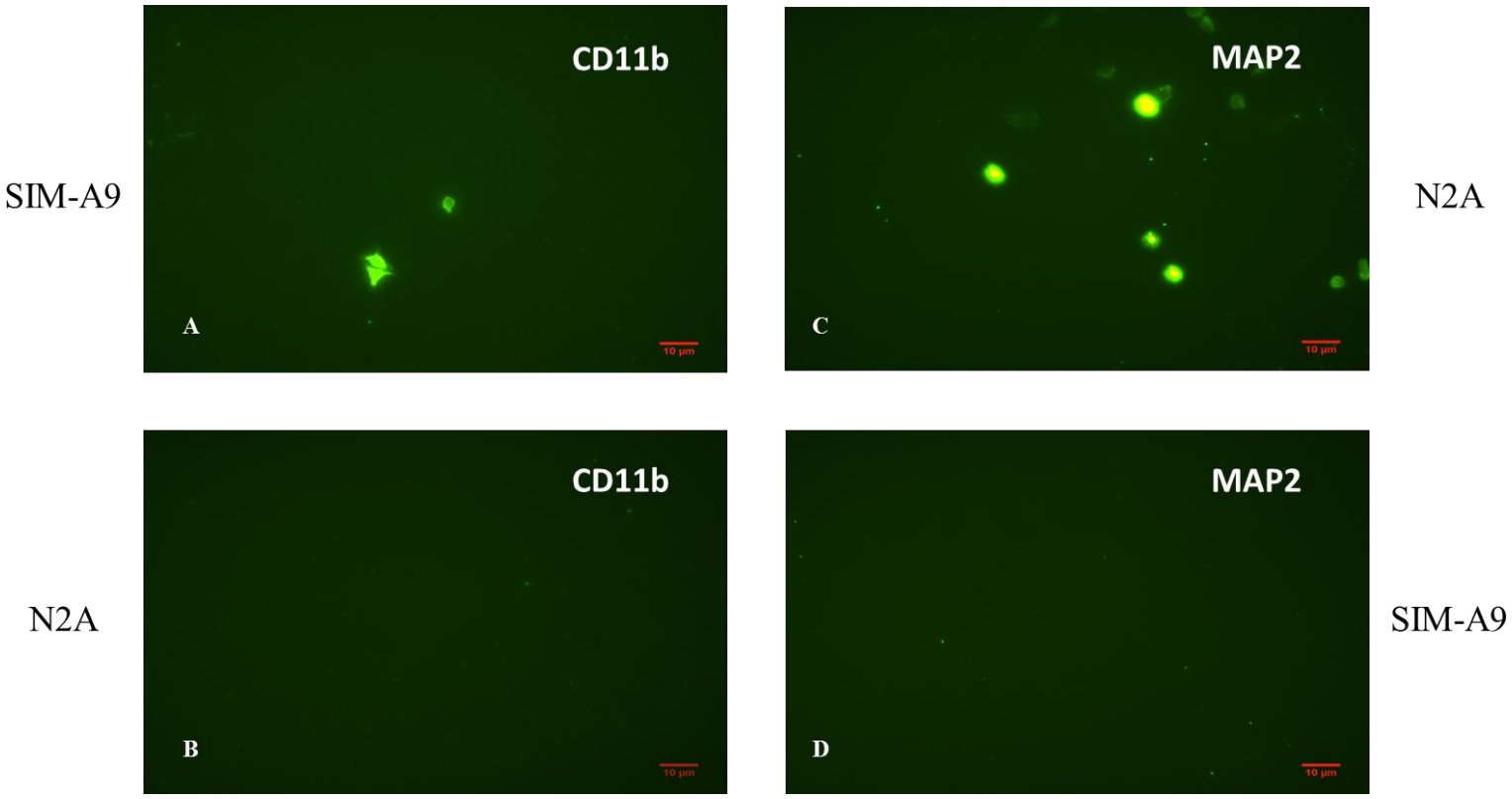

Figure 11. Confirmation of cell types by Immunostaining. SIM-A9 microglia stain positive for the known microglia marker CD11b (A), while staining negative for the known neuronal marker MAP2 (D). N2A neurons stain positive for the known neuronal marker MAP2 (C), while staining negative for the known microglia marker CD11b (B) (Original magnification x400).

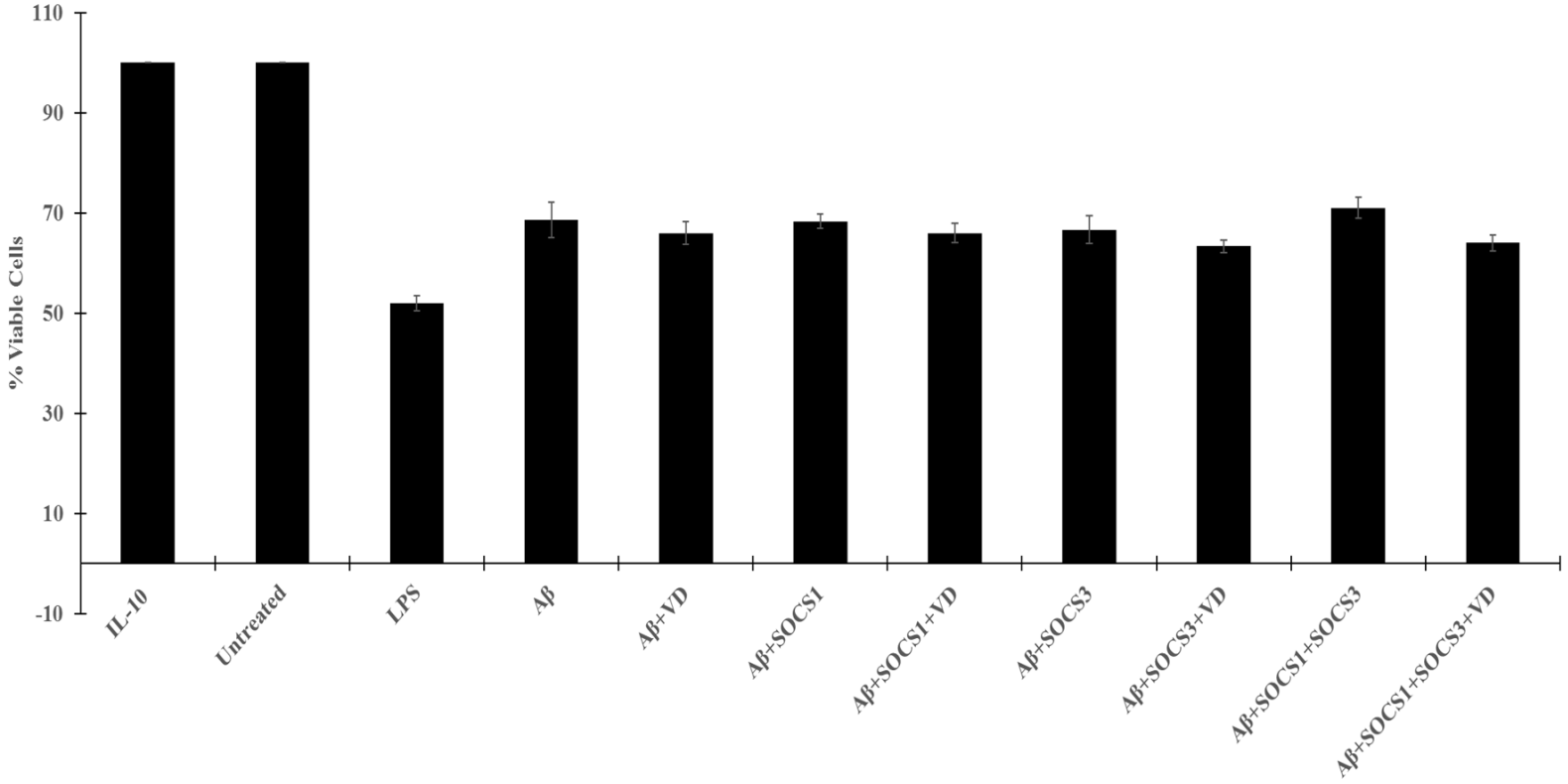

Figure 12. Aβ42, 1,25-(OH)2VD, and SOCS mimetics minimally impact cell viability compared to LPS treatment in a co-culture model. Microglia were treated with IL-10 (100ng/mL), LPS (100 ng/mL), Aβ42 (20 μM), SOCS1 mimetic (35 μM), SOCS3 mimetic (35 μM), and 1,25-(OH)2VD (20 μM). Neurons were stained with trypan blue in a ratio of 1:2 respectively. Dead neurons were stained blue while live neurons remained colorless. All significance (*) was performed using an ANOVA ($p<0.05$). The graph represents three individual repeated experiments.

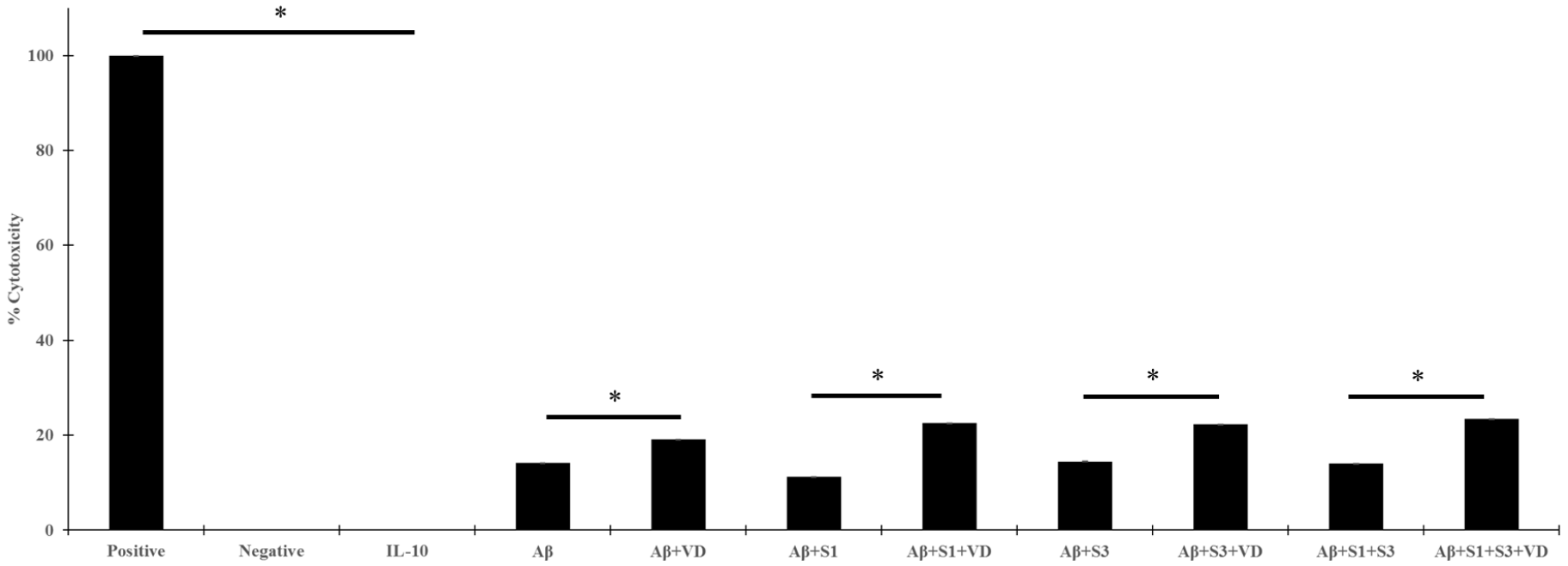

Figure 13. 1,25-(OH)2VD treatment is accompanied by increased cytotoxicity in co-cultures. Microglia were treated with IL-10 (100ng/mL), LPS (100 ng/mL), Aβ42 (20 µM), SOCS1 mimetic (35 µM), SOCS3 mimetic (35 µM), and 1,25-(OH)2VD (20 µM). After 24 hours of incubation, neuronal supernatant was collected and tested for the presence of LDH using a LDH cytotoxicity assay. For maximum release of LDH (positive control) by neurons, 20 µL of Triton X-100 was added to neurons. Minimum release was determined by collecting supernatant of untreated neurons. After 24 hours supernatant was collected and put onto a 96 well plate. Following addition of LDH reaction solution, optical density values were gathered and converted to percent cytotoxicity. Each 1,25-(OH)2VD treatment group had a significant rise in cytotoxicity compared to treatment groups lacking 1,25-(OH)2VD. All significance (*) was performed using an ANOVA ($p<0.05$). The graph represents three individual repeated experiments.

References

1. Asuni, A. A., Perry, V. H., & O'Connor, V. (2010). Change in tau phosphorylation associated with neurodegeneration in the ME7 model of prion disease. *Biochemical Society Transactions, 38*(2), 545-551. doi:10.1042/BST0380545 [doi]
2. Berlato, C., Cassatella, M. A., Kinjyo, I., Gatto, L., Yoshimura, A., & Bazzoni, F. (2002). Involvement of suppressor of cytokine signaling-3 as a mediator of the inhibitory effects of IL-10 on lipopolysaccharide-induced macrophage activation. *Journal of Immunology (Baltimore, Md.: 1950), 168*(12), 6404-6411.
3. Bibl, M., Esselmann, H., & Wiltfang, J. (2012). Neurochemical biomarkers in alzheimer's disease and related disorders. *Therapeutic Advances in Neurological Disorders, 5*(6), 335-348. doi:10.1177/1756285612455367 [doi]
4. Boontanrart, M., Hall, S. D., Spanier, J. A., Hayes, C. E., & Olson, J. K. (2016). Vitamin D3 alters microglia immune activation by an IL-10 dependent SOCS3 mechanism. *Journal of Neuroimmunology, 292*, 126-136. doi:10.1016/j.jneuroim.2016.01.015 [doi]
5. Cai, H., Wang, Y., McCarthy, D., Wen, H., Borchelt, D. R., Price, D. L., et al. (2001). BACE1 is the major beta-secretase for generation of abeta peptides by neurons. *Nature Neuroscience, 4*(3), 233-234. doi:10.1038/85064 [doi]
6. Cardenas-Aguayo Mdel, C., Gomez-Virgilio, L., DeRosa, S., & Meraz-Rios, M. A. (2014). The role of tau oligomers in the onset of alzheimer's disease neuropathology. *ACS Chemical Neuroscience, 5*(12), 1178-1191. doi:10.1021/cn500148z [doi]
7. Chow, V. W., Savonenko, A. V., Melnikova, T., Kim, H., Price, D. L., Li, T., et al. (2010). Modeling an anti-amyloid combination therapy for alzheimer's disease. *Science Translational Medicine, 2*(13), 13ra1. doi:10.1126/scitranslmed.3000337 [doi]
8. Combs, C. K., Karlo, J. C., Kao, S. C., & Landreth, G. E. (2001). Beta-amyloid stimulation of microglia and monocytes results in TNFalpha-dependent expression of inducible nitric oxide synthase and neuronal apoptosis. *The Journal of Neuroscience : The Official Journal of the Society for Neuroscience, 21*(4), 1179-1188. doi:21/4/1179 [pii]
9. Coulson, D. T., Beyer, N., Quinn, J. G., Brockbank, S., Hellemans, J., Irvine, G. B., et al. (2010). BACE1 mRNA expression in alzheimer's disease postmortem brain tissue. *Journal of Alzheimer's Disease : JAD, 22*(4), 1111-1122. doi:10.3233/JAD-2010-101254 [doi]

10. Deane, R., Bell, R. D., Sagare, A., & Zlokovic, B. V. (2009). Clearance of amyloid-beta peptide across the blood-brain barrier: Implication for therapies in alzheimer's disease. *CNS & Neurological Disorders Drug Targets, 8*(1), 16-30.
11. Ding, Y., Chen, D., Tarcsafalvi, A., Su, R., Qin, L., & Bromberg, J. S. (2003). Suppressor of cytokine signaling 1 inhibits IL-10-mediated immune responses. *Journal of Immunology (Baltimore, Md.: 1950), 170*(3), 1383-1391.
12. Friedrich, R. P., Tepper, K., Ronicke, R., Soom, M., Westermann, M., Reymann, K., et al. (2010). Mechanism of amyloid plaque formation suggests an intracellular basis of abeta pathogenicity. *Proceedings of the National Academy of Sciences of the United States of America, 107*(5), 1942-1947. doi:10.1073/pnas.0904532106 [doi]
13. Glenner, G. G., & Wong, C. W. (1984). Alzheimer's disease: Initial report of the purification and characterization of a novel cerebrovascular amyloid protein. 1984. *Biochemical and Biophysical Research Communications, 425*(3), 534-539. doi:10.1016/j.bbrc.2012.08.020 [doi]
14. Haass, C., & Selkoe, D. J. (2007). Soluble protein oligomers in neurodegeneration: Lessons from the alzheimer's amyloid beta-peptide. *Nature Reviews.Molecular Cell Biology, 8*(2), 101-112. doi:nrm2101 [pii]
15. Harms, L. R., Burne, T. H., Eyles, D. W., & McGrath, J. J. (2011). Vitamin D and the brain. *Best Practice & Research.Clinical Endocrinology & Metabolism, 25*(4), 657-669. doi:10.1016/j.beem.2011.05.009 [doi]
16. Hebert, L. E., Weuve, J., Scherr, P. A., & Evans, D. A. (2013). Alzheimer disease in the united states (2010-2050) estimated using the 2010 census. *Neurology, 80*(19), 1778-1783. doi:10.1212/WNL.0b013e31828726f5 [doi]
17. Hebert, S. S., Horre, K., Nicolai, L., Papadopoulou, A. S., Mandemakers, W., Silahtaroglu, A. N., et al. (2008). Loss of microRNA cluster miR-29a/b-1 in sporadic alzheimer's disease correlates with increased BACE1/beta-secretase expression. *Proceedings of the National Academy of Sciences of the United States of America, 105*(17), 6415-6420. doi:10.1073/pnas.0710263105 [doi]
18. Heneka, M. T., Carson, M. J., El Khoury, J., Landreth, G. E., Brosseron, F., Feinstein, D. L., et al. (2015). Neuroinflammation in alzheimer's disease. *The Lancet.Neurology, 14*(4), 388-405. doi:10.1016/S1474-4422(15)70016-5 [doi]
19. Holick, M. F. (2009). Vitamin D status: Measurement, interpretation, and clinical application. *Annals of Epidemiology, 19*(2), 73-78. doi:10.1016/j.annepidem.2007.12.001 [doi]
20. Hong, H., Kim, B. S., & Im, H. I. (2016). Pathophysiological role of neuroinflammation in neurodegenerative diseases and psychiatric disorders. *International Neurourology Journal, 20*(Suppl 1), S2-7. doi:10.5213/inj.1632604.302 [doi]
21. Hubo, M., Trinschek, B., Kryczanowsky, F., Tuettenberg, A., Steinbrink, K., & Jonuleit, H. (2013). Costimulatory molecules on immunogenic versus tolerogenic

human dendritic cells. *Frontiers in Immunology, 4*, 82. doi:10.3389/fimmu.2013.00082 [doi]
22. Joshi, P., Turola, E., Ruiz, A., Bergami, A., Libera, D. D., Benussi, L., et al. (2014). Microglia convert aggregated amyloid-beta into neurotoxic forms through the shedding of microvesicles. *Cell Death and Differentiation, 21*(4), 582-593. doi:10.1038/cdd.2013.180 [doi]
23. Karran, E., Mercken, M., & De Strooper, B. (2011). The amyloid cascade hypothesis for alzheimer's disease: An appraisal for the development of therapeutics. *Nature Reviews.Drug Discovery, 10*(9), 698-712. doi:10.1038/nrd3505 [doi]
24. Kimura, R., Devi, L., & Ohno, M. (2010). Partial reduction of BACE1 improves synaptic plasticity, recent and remote memories in alzheimer's disease transgenic mice. *Journal of Neurochemistry, 113*(1), 248-261. doi:10.1111/j.1471-4159.2010.06608.x [doi]
25. Lawrence, T. (2009). The nuclear factor NF-kappaB pathway in inflammation. *Cold Spring Harbor Perspectives in Biology, 1*(6), a001651. doi:10.1101/cshperspect.a001651 [doi]
26. Lefebvre d'Hellencourt, C., Montero-Menei, C. N., Bernard, R., & Couez, D. (2003). Vitamin D3 inhibits proinflammatory cytokines and nitric oxide production by the EOC13 microglial cell line. *Journal of Neuroscience Research, 71*(4), 575-582. doi:10.1002/jnr.10491 [doi]
27. Lehnardt, S., Lachance, C., Patrizi, S., Lefebvre, S., Follett, P. L., Jensen, F. E., et al. (2002). The toll-like receptor TLR4 is necessary for lipopolysaccharide-induced oligodendrocyte injury in the CNS. *The Journal of Neuroscience : The Official Journal of the Society for Neuroscience, 22*(7), 2478-2486. doi:20026268 [doi]
28. Lue, L. F., Kuo, Y. M., Beach, T., & Walker, D. G. (2010). Microglia activation and anti-inflammatory regulation in alzheimer's disease. *Molecular Neurobiology, 41*(2-3), 115-128. doi:10.1007/s12035-010-8106-8 [doi]
29. Maezawa, I., Zimin, P. I., Wulff, H., & Jin, L. W. (2011). Amyloid-beta protein oligomer at low nanomolar concentrations activates microglia and induces microglial neurotoxicity. *The Journal of Biological Chemistry, 286*(5), 3693-3706. doi:10.1074/jbc.M110.135244 [doi]
30. Martorana, A., Bulati, M., Buffa, S., Pellicano, M., Caruso, C., Candore, G., et al. (2012). Immunosenescence, inflammation and alzheimer's disease. *Longevity & Healthspan, 1*, 8-2395-1-8. eCollection 2012. doi:10.1186/2046-2395-1-8 [doi]
31. McGeer, P. L., & McGeer, E. G. (2013). The amyloid cascade-inflammatory hypothesis of alzheimer disease: Implications for therapy. *Acta Neuropathologica, 126*(4), 479-497. doi:10.1007/s00401-013-1177-7 [doi]
32. Mills, J., & Reiner, P. B. (1999). Mitogen-activated protein kinase is involved in N-methyl-D-aspartate receptor regulation of amyloid precursor protein cleavage. *Neuroscience, 94*(4), 1333-1338. doi:S0306-4522(99)00381-4 [pii]

33. Morris, J. C., Roe, C. M., Xiong, C., Fagan, A. M., Goate, A. M., Holtzman, D. M., et al. (2010). APOE predicts amyloid-beta but not tau alzheimer pathology in cognitively normal aging. *Annals of Neurology, 67*(1), 122-131. doi:10.1002/ana.21843 [doi]
34. Murphy, M. P., & LeVine, H.,3rd. (2010). Alzheimer's disease and the amyloid-beta peptide. *Journal of Alzheimer's Disease : JAD, 19*(1), 311-323. doi:10.3233/JAD-2010-1221 [doi]
35. Nagamoto-Combs, K., Kulas, J., & Combs, C. K. (2014). A novel cell line from spontaneously immortalized murine microglia. *Journal of Neuroscience Methods, 233*, 187-198. doi:10.1016/j.jneumeth.2014.05.021 [doi]
36. Nair, S., Pandey, A. D., & Mukhopadhyay, S. (2011). The PPE18 protein of mycobacterium tuberculosis inhibits NF-kappaB/rel-mediated proinflammatory cytokine production by upregulating and phosphorylating suppressor of cytokine signaling 3 protein. *Journal of Immunology (Baltimore, Md.: 1950), 186*(9), 5413-5424. doi:10.4049/jimmunol.1000773 [doi]
37. Niemand, C., Nimmesgern, A., Haan, S., Fischer, P., Schaper, F., Rossaint, R., et al. (2003). Activation of STAT3 by IL-6 and IL-10 in primary human macrophages is differentially modulated by suppressor of cytokine signaling 3. *Journal of Immunology (Baltimore, Md.: 1950), 170*(6), 3263-3272.
38. O'Brien, R. J., & Wong, P. C. (2011). Amyloid precursor protein processing and alzheimer's disease. *Annual Review of Neuroscience, 34*, 185-204. doi:10.1146/annurev-neuro-061010-113613 [doi]
39. Paquet, D., Kwart, D., Chen, A., Sproul, A., Jacob, S., Teo, S., et al. (2016). Efficient introduction of specific homozygous and heterozygous mutations using CRISPR/Cas9. *Nature, 533*(7601), 125-129. doi:10.1038/nature17664 [doi]
40. Pearson, H. A., & Peers, C. (2006). Physiological roles for amyloid beta peptides. *The Journal of Physiology, 575*(Pt 1), 5-10. doi:jphysiol.2006.111203 [pii]
41. Plant, L. D., Boyle, J. P., Smith, I. F., Peers, C., & Pearson, H. A. (2003). The production of amyloid beta peptide is a critical requirement for the viability of central neurons. *The Journal of Neuroscience : The Official Journal of the Society for Neuroscience, 23*(13), 5531-5535. doi:23/13/5531 [pii]
42. Puzzo, D., Privitera, L., Leznik, E., Fa, M., Staniszewski, A., Palmeri, A., et al. (2008). Picomolar amyloid-beta positively modulates synaptic plasticity and memory in hippocampus. *The Journal of Neuroscience : The Official Journal of the Society for Neuroscience, 28*(53), 14537-14545. doi:10.1523/JNEUROSCI.2692-08.2008 [doi]
43. Puzzo, D., Lee, L., Palmeri, A., Calabrese, G., & Arancio, O. (2014). Behavioral assays with mouse models of Alzheimer's disease: practical considerations and guidelines. *Biochemical Pharmacology, 88*(4), 450–467. http://doi.org/10.1016/j.bcp.2014.01.011
44. Reichard, A. C., Cheemarla, N. R., & Bigley, N. J. (2015). SOCS1/3 expression levels in HSV-1-infected, cytokine-polarized and -unpolarized

macrophages. *Journal of Interferon & Cytokine Research : The Official Journal of the International Society for Interferon and Cytokine Research, 35*(1), 32-41. doi:10.1089/jir.2013.0070 [doi]
45. Ring, S., Weyer, S. W., Kilian, S. B., Waldron, E., Pietrzik, C. U., Filippov, M. A., et al. (2007). The secreted beta-amyloid precursor protein ectodomain APPs alpha is sufficient to rescue the anatomical, behavioral, and electrophysiological abnormalities of APP-deficient mice. *The Journal of Neuroscience : The Official Journal of the Society for Neuroscience, 27*(29), 7817-7826. doi:27/29/7817 [pii]
46. Sengupta, U., Nilson, A. N., & Kayed, R. (2016). The role of amyloid-beta oligomers in toxicity, propagation, and immunotherapy. *Ebiomedicine, 6*, 42-49. doi:S2352-3964(16)30121-9 [pii]
47. Simic, G., Babic Leko, M., Wray, S., Harrington, C., Delalle, I., Jovanov-Milosevic, N., et al. (2016). Tau protein hyperphosphorylation and aggregation in alzheimer's disease and other tauopathies, and possible neuroprotective strategies. *Biomolecules, 6*(1), 6. doi:10.3390/biom6010006 [doi]
48. Smith, P., Al Hashimi, A., Girard, J., Delay, C., & Hebert, S. S. (2011). In vivo regulation of amyloid precursor protein neuronal splicing by microRNAs. *Journal of Neurochemistry, 116*(2), 240-247. doi:10.1111/j.1471-4159.2010.07097.x [doi]
49. Strebovsky, J., Walker, P., Lang, R., & Dalpke, A. H. (2011). Suppressor of cytokine signaling 1 (SOCS1) limits NFkappaB signaling by decreasing p65 stability within the cell nucleus. *FASEB Journal : Official Publication of the Federation of American Societies for Experimental Biology, 25*(3), 863-874. doi:10.1096/fj.10-170597 [doi]
50. Tak, P. P., & Firestein, G. S. (2001). NF-kappaB: A key role in inflammatory diseases. *The Journal of Clinical Investigation, 107*(1), 7-11. doi:10.1172/JCI11830 [doi]
51. Tang, Y., & Le, W. (2016). Differential roles of M1 and M2 microglia in neurodegenerative diseases. *Molecular Neurobiology, 53*(2), 1181-1194. doi:10.1007/s12035-014-9070-5 [doi]
52. Tang, Y., & Le, W. (2016). Differential roles of M1 and M2 microglia in neurodegenerative diseases. *Molecular Neurobiology, 53*(2), 1181-1194. doi:10.1007/s12035-014-9070-5 [doi]
53. Tang, Y., & Le, W. (2016). Differential roles of M1 and M2 microglia in neurodegenerative diseases. *Molecular Neurobiology, 53*(2), 1181-1194. doi:10.1007/s12035-014-9070-5 [doi]
54. Tapiola, T., Alafuzoff, I., Herukka, S. K., Parkkinen, L., Hartikainen, P., Soininen, H., et al. (2009). Cerebrospinal fluid {beta}-amyloid 42 and tau proteins as biomarkers of alzheimer-type pathologic changes in the brain. *Archives of Neurology, 66*(3), 382-389. doi:10.1001/archneurol.2008.596 [doi]
55. Walter, S., Letiembre, M., Liu, Y., Heine, H., Penke, B., Hao, W., et al. (2007). Role of the toll-like receptor 4 in neuroinflammation in alzheimer's disease. *Cellular Physiology and Biochemistry : International Journal of*

Experimental Cellular Physiology, Biochemistry, and Pharmacology, 20(6), 947-956. doi:10.1159/000110455 [doi]
56. Ward, M. W., Concannon, C. G., Whyte, J., Walsh, C. M., Corley, B., & Prehn, J. H. (2010). The amyloid precursor protein intracellular domain(AICD) disrupts actin dynamics and mitochondrial bioenergetics. *Journal of Neurochemistry, 113*(1), 275-284.
57. Wobke, T. K., Sorg, B. L., & Steinhilber, D. (2014). Vitamin D in inflammatory diseases. *Frontiers in Physiology, 5*, 244. doi:10.3389/fphys.2014.00244 [doi]
58. Yin, K., & Agrawal, D. K. (2014). Vitamin D and inflammatory diseases. *Journal of Inflammation Research, 7*, 69-87. doi:10.2147/JIR.S63898 [doi]
59. Yin, K., & Agrawal, D. K. (2014). Vitamin D and inflammatory diseases. *Journal of Inflammation Research, 7*, 69-87. doi:10.2147/JIR.S63898 [doi]
60. Yoshimura, A., Naka, T., & Kubo, M. (2007). SOCS proteins, cytokine signalling and immune regulation. *Nature Reviews.Immunology, 7*(6), 454-465. doi:nri2093 [pii]
61. Yu, H., Pardoll, D., & Jove, R. (2009). STATs in cancer inflammation and immunity: A leading role for STAT3. *Nature Reviews.Cancer, 9*(11), 798-809. doi:10.1038/nrc2734 [doi]
62. Zhang, Y. W., Thompson, R., Zhang, H., & Xu, H. (2011). APP processing in alzheimer's disease. *Molecular Brain, 4*, 3-6606-4-3. doi:10.1186/1756-6606-4-3 [doi]

Appendix

Table 1. Concentration of IL-10 from microglia supernatant
as detected by ELISA (pg/mL)

Treatment	Trial 1 (pg/mL	Trial 2 (pg/mL)	Trial 3 (pg/mL)	Average (pg/mL)	SEM
Negative	28	41	5	24.7	+/- 10.5
IL-10	20890	21360	15090	19113.3	+/- 2016.2
VD	15	175	45	78.3	+/- 49.1
LPS	0	0	0	0	+/- 0
LPS+VD	650	140	135	308.3	+/- 170.8
IFN-γ	0	0	0	0	+/- 0
IFN-γ+ VD	70	290	25	128.3	+/- 81.9
LPS+ IFN-γ	0	0	0	0	+/- 0
LPS+ IFN-γ+ VD	115	360	535	336.6	+/- 121.8
SOCS3	0	0	0	0	+/- 0
SOCS3 + VD	0	0	0	0	+/- 0
LPS+ IFN-γ+SOCS3	0	0	0	0	+/- 0
LPS+ IFN-γ+SOCS3+VD	0	0	0	0	+/- 0
SOCS1+SOCS3	0	0	0	0	+/- 0
SOCS1+SOCS3+VD	0	0	0	0	+/- 0
LPS+IFN-γ+SOCS1+SOCS3	0	0	0	0	+/- 0
LPS+IFN-γ+SOCS1+SOCS3+VD	0	0	0	0	+/- 0

Table 2. Concentration of TNF-α from Supernatant as detected by ELISA (pg/mL)

Treatment	Trial 1 (pg/mL)	Trial 2 (pg/mL)	Trial 3 (pg/mL)	Average (pg/ml)	SEM
Negative	355	190	190	245	+/- 0.011
IL-10	265	325	255	282	+/- 0.004
VD	325	255	325	302	+/- 0.005
LPS	4673	4760	4760	4731	+/- 0.006
LPS+VD	4760	4760	4625	4715	+/- 0.009
IFN-γ	890	740	655	762	+/- 0.014
IFN-γ + VD	715	760	730	735	+/- 0.003
LPS + IFN-γ	4760	4760	4530	4683	+/- 0.015
LPS + IFN-γ + VD	4760	4500	4760	4673	+/- 0.017
SOCS3	0	0	0	0	+/- 0
SOCS3 + VD	0	0	0	0	+/- 0
LPS + IFN-γ+ SOCS3	3300	2650	2645	2865	+/- 0.044
LPS+ IFN-γ + SOCS3 + VD	1380	1540	1385	1435	+/- 0.011
SOCS1	35	10	10	18.3	+/- 0.002
SOCS1 + VD	25	15	20	20	+/- 0.001
SOCS1 +LPS + IFN-γ	4680	4135	4025	4280	+/- 0.041
SOCS1 + LPS + IFN-γ + VD	530	480	460	490	+/- 0.004
SOCS1+SOCS3	10	5	5	7	+/- 0.0002
SOCS1+SOCS3+VD	5	5	0	3	+/- 0.0002
LPS+IFN-γ+SOCS1+SOCS3	1570	1700	1485	1585	+/- 0.009
LPS+IFN-γ+SOCS1+SOCS3+VD	250	410	390	350	0.007

Table 3. Concentration of TNF-α from microglia supernatant following treatment with Aβ42 as detected by ELISA

Treatment	Trial 1 (pg/mL)	Trial 2 (pg/mL)	Trial 3 (pg/mL)	Average (pg/mL)	SEM
LPS	4550	4265	4740	4518	+/- 0.028
Negative	0	0	0	0	0
AB	1195	1140	920	1085	+/- 0.017
AB + SOCS3	95	100	95	97	+/- 0.0003
AB + SOCS1	910	985	1170	1022	+/- 0.015
AB+SOCS1+ SOCS3	**60**	**10**	**15**	**28**	**+/- 0.002**
AB + VD	880	875	915	890	+/- 0.003
AB + SOCS3 + VD	95	75	70	80	+/- 0.002
AB + SOCS1 + VD	125	125	125	125	+/- 2.45E-18
AB+SOCS1+ SOCS3+VD	**10**	**5**	**5**	**7**	**+/- 0.0002**

Table 4. Concentration of IL-10 from microglia supernatant following treatment with Aβ42 detected by ELISA

Treatment	Trial 1 (pg/mL)	Trial 2 (pg/mL)	Trial 3 (pg/mL)	Average (pg/mL)	SEM
LPS	0	0	0	0	0
Negative	0	0	0	0	0
Aβ	0	0	0	0	0
Aβ + SOCS3	0	0	0	0	0
Aβ + SOCS1	25	0	0	8.33	+/- 0.002
Aβ + SOCS1+ SOCS3					
Aβ + VD	0	0	0	0	0
Aβ + SOCS3 + VD	0	0	0	0	0
Aβ + SOCS1 + VD	0	40	0	13.3	+/- 0.002
Aβ+SOCS1+ SOCS3+VD					

Table 5. TNF-α concentration from neuronal supernatant collected from co-cultures and measured by ELISA

Treatment	Trial 1 (pg/mL)	Trial 2 (pg/mL)	Trial 3 (pg/mL)	Average (pg/mL)	SEM
IL-10	0	0	0	0	0
LPS	2660	2560	2615	2612	+/- 0.004
Negative	20	15	0	12	+/- 0.0009
Aβ	660	700	690	683	+/- 0.002
Aβ + VD	110	95	55	87	+/- 0.002
Aβ + SOCS1	600	560	505	555	+/- 0.004
Aβ + SOCS1 + VD	25	50	40	38	+/- 0.001
Aβ + SOCS3	50	115	100	88	+/- 0.003
Aβ + SOCS3 + VD	0	0	5	2	+/- 0.0002
Aβ + SOCS1+ SOCS3	5	0	5	3	+/- 0.0002
Aβ+SOCS1+ SOCS3+VD	5	0	0	2	+/- 0.0002